Università della Calabria

Dottorato di Ricerca in
Scienze e Ingegneria dell'Ambiente, delle Costruzioni e dell'Energia

Tesi

Definition and application of methodological protocols for the conservation and protection of Cultural Heritage: case studies

Settore Scientifico Disciplinare GEO/09

Supervisori

Mauro F. La Russa

Co-Supervisori

Antonio Costanzo

Maria F. Buongiorno

Candidato

Antonio Donato

Ciclo XXXVI

Il Coordinatore del Corso di Dottorato

Salvatore Critelli

Salvatore Critelli
15.04.2024 11:40:35
GMT+02:00

A.A. 2020-2023

Table of Contents

Abstract

This PhD thesis aims to validate a multidisciplinary approach for preventive conservation of cultural heritage as a good practice.
For the purpose of this research, two important pilot sites were chosen in the Calabria region: Cosenza Cathedral (Cosenza, South Italy) and Gerace Cathedral (Reggio Calabria, South Italy).
Cosenza Cathedral represents an important part of the Calabrian cultural asset. It received the status of UNESCO World Heritage Site for being "Heritage Witness to a Culture of Peace" on 12 October 2011. This is the first award given by UNESCO to the Calabria region. A collaboration between Superintendence of Archeology, Fine Arts and Landscape for the Province of Cosenza and University of Calabria occurred on the occasion of the 8th centenary since its consecration by Emperor Frederick II.
This collaboration was aimed to study the state of conservation of Cathedral, and to evaluate the main alteration and degradation phenomena undergoing. In particular, different decay phenomena affecting the façade were assessed through the evaluation of the relative damage indices. For this goal, a multidisciplinary approach was applied exploiting both Non-Destructive and Micro-Destructive Techniques (NDTs and MDTs). Such a combination enabled proposing an intervention priority scale useful to institutions for planning subsequent restoration works.
At the same time, a multi-analytical approach was employed for the first time to study the stone materials, wall paintings and related degradation forms in the Cathedral of Gerace. It's the most imposing Norman building in Calabria with an area of around 1898m^2, and has also been declared Architectural Heritage of National Interest. Its construction dates back to the Norman era (between 1085 and 1120), and despite having undergone numerous restorations, the church perfectly preserves its original building materials. In recent decades, the structure has displayed areas with a poor state of conservation. The study was focused on the decay affecting some building materials and provides an understanding and demonstration of the causes of deterioration.
In the framework of the preventive conservation of cultural heritage, the last part of this PhD thesis was focused on the formulation of a protective coating for the safeguard of underwater cultural heritage (UCH). This choice was made considering the abundance in literature of studies on diagnostics in respect to treatments in underwater environment. Furthermore, in the recent decades, there has been a growing interest in studying decay phenomena and innovative approaches for UCH protection and in-situ preservation, as outlined in the UNESCO Convention on the Protection of Underwater Cultural Heritage held on November 2nd, 2001. This work is a result of technologic and scientific exchange between the University of Calabria (Italy) and Synpo akciova spolecnost (Czech Republic) in the framework of the TECTONIC project (EU-H2020-MSCA-RISE-2019-873132-TECTONIC TEchnological Consortium TO develop sustaiNabIlity of underwater Cultural heritage).
The following introductory chapter provides a general overview of cultural heritage, the importance of its safeguard and the different approaches to it.

Introduction

Cultural heritage can be defined as artefacts, monuments, a group of buildings and sites, museums, that have a diversity of values including symbolic, historic, artistic, aesthetic, ethnological or anthropological, scientific and social significance. It's possible to distinguish between tangible heritage (movable, immobile and underwater) and intangible cultural heritage (ICH), that are embedded into cultural, and natural heritage artefacts, sites or monuments. The definition excludes ICH related to other cultural domains such as festivals, celebration etc., meanwhile it covers industrial Heritage and cave paintings [1]. It embodies the collective memory and self-perception of a society [2]. Additionally, it holds a perspective that transcends borders, forming a concern that pertains to humanity as a whole. This is due to the fact that the cultural heritage of any nation can be viewed as an integral component of the global cultural heritage [3]. The act of preserving cultural heritage is regarded as a moral obligation within societies, as it serves to uphold and reinforce a nation's sense of identity and its comprehension of its history. In a broader sense, the preservation of cultural heritage is geared toward ensuring the continuation of the cultural legacy shared by all of humanity [4]. The preserved cultural artifacts spanning various epochs underscore the significance societies attribute to elements from both their historical and contemporary cultures. All manifestations of culture originate in the present, and if they are deemed valuable and conserved, they subsequently transition into representatives of past cultural epochs [5].

Preserving and safeguarding cultural heritage is essential for future generations to appreciate and learn from the past. However, cultural heritage is vulnerable to natural disasters, urbanization, conflict, and neglect, and therefore, it requires careful management and conservation efforts to ensure its survival.

The conservation of cultural heritage involves actions aimed at extending the life of cultural heritage while reinforcing its meaningful heritage messages and values. In the field of cultural property, the aim of conservation is to keep the cultural and physical characteristics of the object and guarantee that its value is not diminished in time, outlasting human lifetime [6]. Its definition derives from the set of terms "*restoration*", "*remedial conservation*", and "*preventive conservation*" [7].

Remedial conservation refers to all actions taken to stabilize or slowdown the deterioration of the heritage. These actions are normally carried out only when the loss of cultural asset may happen in a short-timed window, with a chance of altering the appearance of an item. The type of remedial conservation undertake depends on nature and material the heritage is made of.
In the scientific panorama there are different examples of remedial conservation: textiles [8], desalination of ceramics [9], de-acidification of paper [10], dehydration of wet archaeological materials, stabilization of corroded metals, consolidation of mural paintings [11], removing weeds from mosaics [12].

Restoration takes place only when the heritage has lost part of its former significance or function due to alteration or deterioration. In the majority of cases, they alter the appearance of the heritage. It involves all actions directly applied to a single and stable item aimed at facilitating its appreciation, understanding and use, such as integration and replacement of non-original elements, reconstruction [7].

Preventive conservation refers to all the actions aimed to mitigate deterioration and damage to CH; it's an ongoing process that extends throughout the lifespan of cultural assets and persists beyond interventive treatment. procedures. Unlike remedial conservation and restoration, preventive conservation doesn't intervene directly on the fabric of the heritage [13].

The deterioration of cultural heritage materials stands as one of the foremost menaces to their conservation. Over their lifespan, materials routinely undergo degradation due to exposure to particular environmental circumstances, coupled with chemical, physical, and biological forces. As a result, the aging process significantly impacts the durability and functionality of building materials, potentially leading to irreversible losses if not promptly addressed [14–19].

Throughout the 20th century, a notable shift in international conservation principles has been witnessed [20-22], demonstrating a transition from a reactive to a proactive mindset among heritage preservation experts [23, 24]. The 1999 revision of the Burra Charter even labels maintenance as "essential to conservation" [25]. In 2008, at ICOM-CC 15th Triennial Conference held in New Delhi (2008) [7], the term "preventive conservation" has been defined as "all measures and actions aimed at avoiding and minimizing future deterioration or loss. They are carried out within the context or on the surroundings of an item, but more often a group of items, whatever their age and condition. These measures and actions are indirect – they do not interfere with the materials and structures of the items. They do not modify their appearance".

Preventive conservation embodies a deliberate strategy aimed at achieving a more sustainable safeguarding of architectural heritage. This approach capitalizes on systematic maintenance and regular surveillance of tangible assets to "retard the process of deterioration," thereby enhancing the retention of their cultural significance within society. Within the context of preventive conservation, the strategic planning of maintenance efforts necessitates an in-depth comprehension of the relevant structures, achieved through a comprehensive and multidisciplinary methodology [26]. This all-encompassing process scrutinizes the "effects (damages), the cause and the remedies" [27] of unexpected failures "in the design, construction and use of the buildings" [7], distinct from the natural aging process and decay.
Such an approach facilitates not only preventive conservation tactics and comprehensive restoration endeavors but also the widespread dissemination of cultural assets [20, 22, 28]. Effective preventive conservation hinges on a meticulously structured strategy encompassing diagnostics, restoration, and the continuous maintenance of cultural heritage [29]. Consequently, there is a mounting call to refine diagnostic methodologies and enhance the products utilized in restoration practices to render them better suited for a range of environmental conditions. Simultaneously, an imperative exists to heighten the allure and practicality of cultural heritage to bolster tourism [30]. Esteemed standards, institutions, and experts in the domain universally recognize that the preservation of cultural heritage mandates: alignment with the underlying object to ensure minimal intervention, the potential for reversibility and removal, discernible restoration endeavors, a multidisciplinary approach, and a commitment to sustainability.

The effective management of risks tied to CH entails a spectrum of actions, encompassing planning, monitoring, maintenance, prevention, and restoration. These facets must be meticulously coordinated to curtail the potential for damage or loss of cultural heritage. Deliberate monitoring protocols ought to be instituted at historically or archaeologically significant sites to assess potential deterioration and harm resulting from diverse factors such as external influences or internal

chemical and physical transformations over time [31, 32]. Consequently, the comprehensive process of risk assessment should entail the identification of specific active decay mechanisms coupled with an integrated inquiry that addresses the nature of decay and damage, as well as the underlying mechanisms driving decay phenomena, including kinetics, thermodynamics, and structural factors [33-35].

Following the shift towards a more preventive conservation rather than an active one, also the monitoring and diagnostic techniques have been improved.
In recent decades, structural health monitoring and management of cultural heritage structures are emerging as the main safeguard measures, aiming to assess the actual state of conservation of the structure [36]. Data gathered from monitoring systems are also crucial in devising economical and sustainable maintenance strategies that align with basic preservation principles for historic structures, such as the concept of minimal intervention. Several applications of monitoring techniques to cultural heritage assets are documented in recent literature, including churches [37, 38], towers [39], palaces [40], and even more complex building such as the Roman Arena of Verona [41].

Together with monitoring and diagnostic techniques, non-invasive techniques such as InfraRed Thermography (IRT), Photogrammetry and 3D reconstruction have emerged as invaluable tools in the CH field.
Infrared thermography, a non-invasive technique, has found a significant application in the field of cultural heritage [42-45]. By capturing and visualizing thermal radiation emitted by objects and structures, it offers unique insights into their physical conditions, material composition, and structural integrity [46]. This technology plays a pivotal role in architectural preservation, as it helps detect hidden defects, moisture accumulation, and degradation within historical buildings. Through detailed thermal imaging, conservators can pinpoint areas of concern and implement targeted interventions, ensuring the longevity of the architectural elements [47].
Simultaneously, the fusion of photogrammetric survey and 3D reconstruction has brought about a digital revolution in the study and conservation of cultural artifacts and sites. By analyzing multiple images taken from various angles, photogrammetry meticulously reconstructs three-dimensional models, granting unprecedented accuracy in documenting intricate details [48]. This technique proves particularly advantageous in capturing delicate artifacts and inaccessible areas of heritage sites, ensuring their preservation for posterity. The synergy between photogrammetric data and other methodologies such as laser scanning enhances the fidelity of these reconstructions, offering archaeologists, historians, and conservators, comprehensive insights into architectural intricacies and object dimensions [49-52].
The impact of photogrammetry extends beyond mere documentation. The interactive virtual replicas created through this technology facilitate broader public engagement and educational outreach. These digital recreations enable individuals to explore heritage sites and artifacts with an unprecedented level of immersion, bridging the gap between the past and the present. Moreover, the non-destructive nature of photogrammetry ensures the protection of valuable artifacts and historical structures, making it an essential component of sustainable cultural heritage preservation.
Collectively, the combination of infrared thermography and photogrammetric survey with 3D reconstruction presents a formidable arsenal for safeguarding and understanding our cultural heritage. Infrared thermography's ability to unveil hidden anomalies in architectural structures and artworks, along with photogrammetry's prowess in creating precise digital replicas, redefine the methodologies employed by archaeologists, conservators, and researchers. As technology continues

to advance, these tools will undoubtedly evolve, further enriching our appreciation of the past and strengthening our commitment to its preservation for generations to come.
In the context of preventive conservation, it's also important to have a deep knowledge of stone properties, decay forms and processes occurred on the case study. MDTs have emerged as crucial tools in the realm of cultural heritage analysis, offering invaluable insights while minimizing irreversible damage to precious artifacts and structures. These techniques, including micro-sampling, thin sectioning, and microchemical analysis, enable researchers to delve deep into the composition, structure, and historical context of materials without compromising their integrity [53-55]. In archaeological studies, these methods aid in identifying the origins of raw materials used in pottery, ceramics, and metals, shedding light on ancient trade routes and cultural interactions. Additionally, MDTs facilitate the authentication of artworks through pigment analysis and examination of underlying layers [56], supporting art historians in unraveling an artwork's evolution over time. By combining scientific rigor with preservation ethics, MDTs bridge the gap between meticulous analysis and responsible conservation, ensuring that our cultural heritage is both understood and safeguarded.

To ensure a comprehensive evaluation of deterioration in stone-built heritage and the subsequent restoration strategy, relying solely on a single NDT or MDT may prove inadequate for obtaining sufficient data. Instead, a more comprehensive approach involving a combination of various NDTs and MDTs should be employed [57-62]. Such combination can furnish insights into different decay forms encountered, both qualitatively and quantitatively, across scales ranging from nanoscale to mesoscale, culminating in a thorough decay assessment. Moreover, this assessment identifies optimal practices for conservation and restoration efforts.

Another important aspect of preventive conservation is the application of a protective coating in order to make the stone more resistant against pollutants, biological growths, and the action of water.
In the last decades, a variety of protective coatings have been developed for the preservation of CH items and to reduce the deterioration rate. The biggest challenge comes up with their development in order to be conform to the accepted standards of restoration [63]. The ideal protective coating should bring: transparency, reversibility, compatibility with the surface, long-term lifetime, easy synthesis, low-cost maintenance, and non-toxicity. Safety and security rules are intended for both operators and object. The synthesis and the application should be totally (or almost) green and risk-free. Same safety and security rules should be followed during the eventual removal of the coating, that should occur by means of non-toxic solvents. Moreover, the original appearance of the object should remain unchanged. Even if this aspect may appear secondary, it gains priority considering the CH environment, further complicating the choice of the coating. To make the situation even harder, even if a product may appear transparent after its application, it can change color due to environment interaction and photo-oxidation processes (i.e., yellowing of the surface). This behavior may be tolerated if the reversibility of the coating is assured; that means the coating may be removed without compromising the CH surface. In the last 30 years the technologies available for developing new coating have significantly improved, together with the science behind it [64].
Starting from '60s, commercial acrylic polymers have been extensively used in the conservation of CH [65] due to their mechanical properties, transparency, stability and water-repellent capability. They have been employed in the formulation of paints and adhesives, as well as coatings for consolidation and protection. The most relevant issue of these polymers is associated to their durability and removability, as they tend to photo-oxidize. It was reported [66] that, under photo-

oxidative process, two of the most used Paraloid polymers, B67 and B72, were impossible to remove from the stone and registered a decrease on the consolidating and hydro-repellent properties.
Nowadays, due to the problems encountered, acrylic polymers are less used as coating on stone.
In recent times, an increasing attention has been family to a particular family of products: nanocomposites [67]. The addition of nanoparticles to silane and siloxane polymers has improved the performance of the coatings on stone, enhancing their resistance against water, biological growth and pollution. Based on the improvement provided by nanoparticles, these coating can be divided into superhydrophobic, and photocatalytic coatings [68].
The super hydrophobicity prevents the adhesion of microorganisms, ensuring their removal. The photocatalytic property induces the decomposition of the polluting agents, inhibiting their accumulation. Hence, it allows their utilization as self-cleaning components and against bacteria proliferation [69].
Among the several types of nanoparticles, TiO_2 holds a center spot. Its self-cleaning capability is connected to the photocatalytic properties of the nanoparticles, and it's possible to improve their performance by optimizing their synthesis process. The main drawback in the application of this nanoparticles is in the color variation inducted by an excess of TiO_2 [70].
The usage of nanoparticle coatings in the cultural heritage field is still limited, although it has brought improvement in the protection of cultural heritage.

In this scientifical context, my PhD research developed and can be summarized in two steps. The first one was aimed to establish the best diagnostic approach to define the state of conservation of Cosenza and Gerace Cathedral, that are two of the most important monuments located in Calabria region. The second one was focused on the development of coatings to preserve the underwater cultural heritage.

In Chapter 1 and Chapter 2, two of the most important building of the Calabrian region (South Italy), from an historical point of view, were studied: the Cosenza Cathedral, UNESCO World Heritage Site since 12 October 2011, and the Gerace Cathedral, declared Architectural Heritage of National Interest. In order to assess the different decay phenomena occurred on the building, a multidisciplinary approach has been applied, involving the combined usage of nondestructive techniques (NDTs) and microdestructive techniques (MDTs). In both cases, the same approach (with different methodologies) has been applied:

- Macroscopical observation;
- Nondestructive techniques (on site);
- Microsampling and mapping;
- Microdestructive techniques (in laboratory);
- Damage analysis;
- Planning of future intervention.

In the context of preventive conservation, Chapter 3 will deal with another aspect of it, that is the application of a protective coating. The choice about this part of my research was guided by several aspects. Even if this case study is related to Underwater Cultural Heritage, the same approach already discussed can be applied. In underwater environment, the decay forms that affect the stone materials may be different from the sub-aerial ones, but the process involved in the diagnostic, conservation and preservation of cultural heritage stays the same [71, 72]. Moreover, there is an

abundance in literature of studies on diagnostics in respect to treatments in underwater environment.
Coatings formulated for sub-aerial conditions usually don't keep the same behavior and properties underwater, requiring different application methods, techniques, and posing new challenging tasks for researchers [73-75].
Although, ideally, a protective coating should be reversible, due to issues outlined above, in the first steps of the research the attention was focused on the formulation of an irreversible epoxy-based coating. Although being permanent, it's a coating that showed good applicability underwater and great mechanical properties in the preliminary tests. Experimentation is still in its early stages and will be improved in the future.

References

[1] UNESCO Institute for Statistics, 2009 UNESCO Framework for Cultural Statistics
[2] W. Welburn, V. Pitchford, C. Alire, M. Brown, K. E. Downing, A. Rivera, J. Welburn, M. Winston, "Memory, Authenticity and Cultural Identity: The Role of Library Programs, Services and Collections in Creating Community", IFLA World Library and Information Congress: 75th IFLA General Conference and Council, 23-27 August 2009, Milan, Italy, 2009, pp. 2-3.
[3] The Hague Convention for the Protection of Cultural Property in the Event of Armed Conflict, 1954, UNESCO, p. 1. https://www.unesco.org/en/legal-affairs/convention-protection-cultural-property-event-armed-conflict-regulations-execution-convention
[4] M. V. Cloonan Michéle, "The Moral Imperative to Preserve", Library trends 55(3), 2007, p. 747.
[5] Wirilander, Heidi. (2012). Preventive Conservation: a Key Method to Ensure Cultural Heritage's Authenticity and Integrity in Preservation Process. e-conservation magazine. 5. 164-176.
[6] https://uis.unesco.org/en/glossary-term/conservation-cultural-heritage
[7] Terminology to characterize the conservation of tangible cultural heritage, Resolution adopted by the ICOM-CC membership at the 15th Triennial Conference New Delhi, 22-26 September 2008, pp. 1-2, 2008
[8] S. Tripa, L. Indrie, F. Tripa, M. Mare. (2023). A review on deterioration of textile cultural heritage objects and sustainable solutions to mitigate the degradation. Industria Textila. 74. 555-563. 10.35530/IT.074.05.2022145
[9] S. Noghani, M. Amiri, M. Emami. (2018). A new approach to the desalination process of archaeological potteries. Mediterranean Archaeology and Archaeometry. 18. 255-267. 10.5281/zenodo.1165366
[10] J. Weng, X. Zhang, M. Jia, J. Zhang, Deacidification of aged papers using dispersion of Ca(OH)2 nanoparticles in subcritical 1,1,1,2-tetrafluoroethane (R134a), Journal of Cultural Heritage, Volume 37, 2019, Pages 137-147, ISSN 1296-2074, https://doi.org/10.1016/j.culher.2018.12.001
[11] D. Chelazzi, G. Poggi, Y. Jaidar, N. Toccafondi, R. Giorgi, P. Baglioni, Hydroxide nanoparticles for cultural heritage: Consolidation and protection of wall paintings and carbonate materials, Journal of Colloid and Interface Science, Volume 392, 2013, Pages 42-49, ISSN 0021-9797, https://doi.org/10.1016/j.jcis.2012.09.069
[12] Elgohary, Y.M., Mansour, M.M.A. & Salem, M.Z.M. Assessment of the potential effects of plants with their secreted biochemicals on the biodeterioration of archaeological stones. Biomass Conv. Bioref. (2022). https://doi.org/10.1007/s13399-022-03300-8
[13] Wirilander, H. (2012). Preventive Conservation: a Key Method to Ensure Cultural Heritage's Authenticity and Integrity in Preservation Process. e-conservation magazine, 6(24)
[14] E.T. Delegou, G. Mourgi, E. Tsilimantou, C. Ioannidis, A. Moropoulou, A multidisciplinary approach for historic buildings diagnosis: the case study of the Kaisariani Monastery, Heritage 2 (2019) 1211–1232, https://doi.org/10.3390/heritage2020079.
[15] A. Moropoulou, K.C. Labropoulos, E.T. Delegou, M. Karoglou, A. Bakolas, Non-destructive techniques as a tool for the protection of built cultural heritage, Constr. Build. Mater. Volume 48 (2013) 1222–1239, https://doi.org/10.1016/j.conbuildmat.2013.03.044.
[16] F. Sandrolini, E. Franzoni, G. Cuppini, L. Caggiati, Materials decay and environmental attack in the Pio Palace at Carpi: a holistic approach for historical architectural surfaces conservation, Build. Environ. Volume 42 (Issue 5) (2007) 1966–1974, https://doi.org/10.1016/j.buildenv.2006.04.021.

[17] F. Sandrolini, E. Franzoni, E. Sassoni, P.P. Diotallevi, The contribution of urban-scale environmental monitoring to materials diagnostics: a study on the Cathedral of Modena (Italy), J. Cult. Herit. Volume 12 (Issue 4) (2011) 441–450, https://doi.org/10.1016/j.culher.2011.04.005;
[18] L. Berto, A. Doria, P. Faccio, A. Saetta, D. Talledo, Vulnerability analysis of built cultural heritage: a multidisciplinary approach for studying the Palladio's Tempietto Barbaro, Int. J. Archit. Herit. 11 (6) (2017) 773–790, https://doi.org/10.1080/15583058.2017.1290853.
[19] E. Spoldi, I. Ippolito, A. Stella, S. Russo, Non-destructive techniques for structural characterization of cultural heritage: a pilot case study, Struct. Control Health Monit. 28 (2021) 12, https://doi.org/10.1002/stc.2820.
[20] ICOMOS. International Charter for the Conservation and Restoration of Monuments and Sites; ICOMOS: Venice, Italy, 1964.
[21] Australia ICOMOS. Australia ICOMOS Guidelines for the Conservation of Places of Cultural Significance ("Burra Charter"); Australia ICOMOS: Burra, Australia, 1979; pp. 1–2.
[22] ICOMOS. The Athens Charter for the Restoration of Historic Monuments—1931. Available online: https://www.icomos.org/en/167-the-athens-charter-for-the-restoration-of-historic-monuments (accessed on 19 July 2023).
[23] Heras Barros, V. Towards a 3D GIS based monitoring tools for Preventive Conservation Management of the World Heritage City of Cuenca; KU Leuven: Leuven, Belgium, 2014.
[24] Stulens, A.; Meul, V.; Lipovec, N.C. Heritage Recording and Information Management as a Tool for Preventive Conservation, Maintenance, and Monitoring: The Approach of Monumentenwacht in the Flemish Region (Belgium). Chang. Over Time 2012, 2, 58–76.
[25] Australia ICOMOS. The Burra Charter: The Australia ICOMOS Charter for Places of Cultural Significance; Australia ICOMOS: Burra, Australia, 1999.
[26] Watt, D. Building Pathology Principles and Practice; Blackwell Publishing: Oxford, UK, 1999; ISBN 9781405111720.
[27] Malcolm, T. Managing Building Pathology and Maintenance; Książek, M., Jerzy, R., Eds.; Warsaw University of Technology: Warsaw, Poland, 2013; ISBN 9788378142157.
[28] Jouan, P.; Hallot, P. Digital Twin: Research Framework to Support Preventive Conservation Policies. Int. J. Geo-Inf. 2020, 9, 228.
[29] Binda, L.; Saisi, A.; Tiraboschi, C. Investigation Procedures for the diagnosis of the historic masonries. Construct. Build. Mater. 2000, 14, 199–233.
[30] Timothy, D.J.; Gyan, P.N. Cultural Heritage and Tourism in the Developing World: A Regional Perspect; Routledge Taylor & Francis Group: Abingdon-on-Thames, UK, 2009; p. 260.
[31] Camuffo, D. Microclimate for Cultural Heritage; Elsevier: Amsterdam, The Netherlands, 1998.
[32] Camuffo, D.; Fassina, V.; Havermans, J. Basic Environmental Mechanisms Affecting Cultural Herit; Nardini Editore: Firenze, Italy, 2010.
[33] Moropoulou, A.; Kioussi, A.; Karoglou, M.; Bakolas, A.; Georgousopoulos, G.; Chronopoulos, M. Innovative protocols for integrated diagnostics on historic materials and structures. In Structural Faults and Repair; Radonjanin, V., Crews, K., Eds.; University of Edinburgh: Edinburgh, UK, 2012; pp. 397–399.
[34] Kioussi, A.; Labropoulos, K.; Karoglou, M.; Moropoulou, A.; Zarnic, R. Recommendations and strategies for the establishment of a guideline for monument documentation harmonized with the existing European standards and codes. J. Geoinf. FCE CTU 2011, 6, 178–184.
[35] Antonelli, F.; Lazzarini, L.; Cancelliere, S.; Tesser, E. Study of the deterioration products, gilding, and polychromy of the stones of the Scuola Grande Di San Marco's façade in Venice. Stud. Conserv. 2016, 61, 74–85.
[36] Rossi, M.; Bournas, D. Structural Health Monitoring and Management of Cultural Heritage Structures: A State-of-the-Art Review. Appl. Sci. 2023, 13, 6450. https://doi.org/10.3390/app13116450
[37] Gentile, C., Ruccolo, A. & Canali, F. Continuous monitoring of the Milan Cathedral: dynamic characteristics and vibration-based SHM. J Civil Struct Health Monit 9, 671–688 (2019). https://doi.org/10.1007/s13349-019-00361-8
[38] R. Alaggio, A. Aloisio, E. Antonacci, R. Cirella, Two-years static and dynamic monitoring of the Santa Maria di Collemaggio basilica, Construction and Building Materials, Volume 268, 2021, 121069, ISSN 0950-0618, https://doi.org/10.1016/j.conbuildmat.2020.121069

[39] Saisi, A., Gentile, C. & Ruccolo, A. Continuous monitoring of a challenging heritage tower in Monza, Italy. J Civil Struct Health Monit 8, 77–90 (2018). https://doi.org/10.1007/s13349-017-0260-5
[40] Cavalagli, N. et al. (2021). Remote Sensing and In-Situ Measurements for the Structural Monitoring of Historical Monuments: The Consoli Palace of Gubbio, Italy. In: Rizzo, P., Milazzo, A. (eds) European Workshop on Structural Health Monitoring. EWSHM 2020. Lecture Notes in Civil Engineering, vol 128. Springer, Cham. https://doi.org/10.1007/978-3-030-64908-1_11
[41] Lorenzoni, F., Casarin, F., Modena, C. et al. Structural health monitoring of the Roman Arena of Verona, Italy. J Civil Struct Health Monit 3, 227–246 (2013). https://doi.org/10.1007/s13349-013-0065-0
[42] F. Mercuri, N. Orazi, U. Zammit, S. Paoloni, M. Marinelli, P.P. Valentini, e-PS 9, 84 (2012)
[43] Jo, H.; Lee, C.H. Quantitative modelling and mapping of blistering zone of the Magoksa Temple stone pagoda (13th century, Republic of Korea) by graduated heating thermography. Infrared Phys. Technol. 2014, 65, 43–50.
[44] Faella, G.; Frunzio, G.; Guadagnuolo, M.; Donadio, A.; Ferri, L. The Church of the Nativity in Bethlehem: Non-destructive tests for the structural knowledge. J. Cult. Herit. 2012, 13, e27–e41.
[45] Becherini, F.; Bernardi, A.; Di Tuccio, M.C.; Vivarelli, A.; Pockelè, L.; De Grandi, S.; Fortuna, S.; Quendolo, A. Microclimatic monitoring for the investigation of the different state of conservation of the stucco statues of the Longobard Temple in Cividale del Friuli (Udine, Italy). J. Cult. Herit. 2016, 18, 375–379.
[46] X. Maldague, Theory and Practice of Infrared Technology for Nondestructive Testing (Wiley, New York, 2011)
[47] F. Mercuri, U. Zammit, N. Orazi, S. Paoloni, M. Marinelli, F. Scudieri, J. Therm. Anal. Calorim. 104, 2 (2011).
[48] K.B. Atkinson, Close-range Photogrammetry and Machine Vision, Whittles Publishing, Scotland, 1996.
[49] E. Berndt, J. Carlos, Cultural heritage in the mature era of computer graphics, IEEE Computer Graphics and Applications 20 (1) (2000) 36e37.
[50] L.G. Desmond, P. Collins, T.G. Negron, J. Callaghan, Gateway into the past: Photogrammetric documentation of the Arch, Labna, Yucatan, Mexico, in: L.P. Barba (Ed.), Antropologia y Tecnica 7 (IIA) (2003) 55e66.
[51] G. Guidi, A. Beraldin, C. Atzeni, High-accuracy 3-D modeling of cultural heritage: the digitizing of Donatello's ''Maddalena'' image, Proc. IEEE Trans. On 13 (3) (2004) 370e380.
[52] M. Pieraccini, G. Guidi, C. Atzeni, 3D digitizing of cultural heritage, Journal of Cultural Heritage 2 (2001) 63e70.
[53] C. Walker, I. Joosten, Introduction: Analysis of Cultural Heritage, in: Microscopy and Microanalysis, 2011, 17 (5), 655-655. doi:10.1017/S1431927611012062
[54] A. Ali, Y.W. Chiang, R.M. Santos, X-ray Diffraction Techniques for Mineral Characterization: A Review for Engineers of the Fundamentals, Applications, and Research Directions. Minerals, 2022, 12, 205. https://doi.org/10.3390/min12020205
[55] A. Alvarez de Buergo, M.P. Lopez-Arce, R. Fort, Ion chromatography to detect salts in stone structures and to assess salt removal methods. EGU General Assembly Conference Abstracts, 2012, vol. 14, p. 1757.
[56] Ricca, M.; Alberghina, M.F.; Randazzo, L.; Schiavone, S.; Donato, A.; Albanese, M.P.; La Russa, M.F. A Combined Non-Destructive and Micro-Destructive Approach to Solving the Forensic Problems in the Field of Cultural Heritage: Two Case Studies. Appl. Sci. 2021, 11, 6951. https://doi.org/10.3390/app11156951
[57] Diz-Mellado, E.; Mascort-Albea, E.J.; Romero-Hernández, R.; Galán-Marín, C.; Rivera-Gómez, C.; Ruiz-Jaramillo, J.; Jaramillo-Morilla, A. Non-destructive testing and Finite Element Method integrated procedure for heritage diagnosis: The Seville Cathedral case study. J. Build. Eng. 2021, 37, 102134, https://doi.org/10.1016/j.jobe.2020.102134.
[58] Chastre, C.; Ludovico-Marques, M. Chapter 13—Nondestructive testing methodology to assess the conservation of historic stone buildings and monuments. In Handbook of Materials Failure Analysis; Makhlouf, A.S.H., Aliofkhazraei, M., Eds.; Butterworth-Heinemann: Oxford, UK, 2018; pp. 255–294, https://doi.org/10.1016/B978-0-08-101928-3.00013-6.
[59] Kilic, G. Using advanced NDT for historic buildings: Towards an integrated multidisciplinary health assessment strategy. J. Cult. Herit. 2015, 16, 526–535, https://doi.org/10.1016/j.culher.2014.09.010.

[60] Bosiljkov, V.; Uranjek, M.; Žarnić, R.; Bokan-Bosiljkov, V. An integrated diagnostic approach for the assessment of historic masonry structures. J. Cult. Herit. 2010, 11, 239–249, https://doi.org/10.1016/j.culher.2009.11.007.
[61] Bosiljkov, V.; Maierhofer, C.; Koepp, C.; Wöstmann, J. Assessment of Structure through Non-Destructive Tests (NDT) and Minor Destructive Tests (MDT) Investigation: Case Study of the Church at Carthusian Monastery at Žiče (SLOVENIA). Int. J. Archit. Herit. 2010, 4, 1–15, doi:10.1080/15583050902731031.
[62] Ricca, M., Alexandrakis, G., Bonazza, A., Bruno, F., Davidde Petriaggi, B., Elkin, D., Lagudi, A., Nicolas, S., Novák, M., Papatheodorou, G., Prieto, J., Ricci, M., Vasilijevic, A., La Russa, M.F. A Sustainable Approach for the Management and Valorization of Underwater Cultural Heritage: New Perspectives from the TECTONIC Project. Sustainability 2020, 12, 5000. https://doi.org/10.3390/su12125000.
[63] Brandi, C. Il Restauro. Teoria e Pratica (1939–1986); Saggi Arte; Editori Riuniti: Roma, Italy, 2009
[64] Artesani, A.; Di Turo, F.; Zucchelli, M.; Traviglia, A. Recent Advances in Protective Coatings for Cultural Heritage–An Overview. Coatings 2020, 10, 217. https://doi.org/10.3390/coatings10030217
[65] Robert L. Feller (1961) NEW SOLVENT-TYPE VARNISHES, Studies in Conservation, 6:sup1, 171-175, DOI: 10.1179/sic.1961.s040
[66] M. Favaro, R. Mendichi, F. Ossola, U. Russo, S. Simon, P. Tomasin, P.A. Vigato, Evaluation of polymers for conservation treatments of outdoor exposed stone monuments. Part I: Photo-oxidative weathering, Polymer Degradation and Stability, Volume 91, Issue 12, 2006, Pages 3083-3096, ISSN 0141-3910, https://doi.org/10.1016/j.polymdegradstab.2006.08.012
[67] P. Munafò, G.B. Goffredo, E. Quagliarini, TiO2-based nanocoatings for preserving architectural stone surfaces: An overview, Construction and Building Materials, Volume 84, 2015, Pages 201-218, ISSN 0950-0618, https://doi.org/10.1016/j.conbuildmat.2015.02.083
[68] Ruffolo S.A., La Russa M.F., Nanostructured Coatings for Stone Protection: An Overview, Frontiers in Materials, 6, 2019, 10.3389/fmats.2019.00147
[69] Wang, R.; Hashimoto, K.; Fujishima, A.; Chikuni, M.; Kojima, E.; Kitamura, A.; Watanabe, T. Photogeneration of highly amphiphilic TiO2 surfaces. Adv. Mater. 1998. https://doi.org/10.1002/(SICI)1521-4095(199801)10:2<135::AID-ADMA135>3.0.CO;2-M
[70] V. Crupi, B. Fazio, A. Gessini, Z. Kis, M.F. La Russa, D. Majolino, C. Masciovecchio, M. Ricca, B. Rossi, S.A. Ruffolo, V. Venuti, TiO2–SiO2–PDMS nanocomposite coating with self-cleaning effect for stone material: Finding the optimal amount of TiO2, Construction and Building Materials, Volume 166, 2018, Pages 464-471, ISSN 0950-0618, https://doi.org/10.1016/j.conbuildmat.2018.01.172
[71] Aloise, P.; Ricca, M.; La Russa, M.; Ruffolo, S.; Belfiore, C.; Padeletti, G.; Crisci, G.M. (2013). Diagnostic analysis of stone materials from underwater excavations: The case study of the Roman archaeological site of Baia (Naples, Italy). Applied Physics A. 114. 655-662. 10.1007/s00339-013-7890-1.
[72] Randazzo, L.; Ricca, M.; Ruffolo, S.; Aquino, M.; Davidde Petriaggi, B.; Enei, F.; La Russa, M.F. An Integrated Analytical Approach to Define the Compositional and Textural Features of Mortars Used in the Underwater Archaeological Site of Castrum Novum (Santa Marinella, Rome, Italy). Minerals 2019, 9, 268. https://doi.org/10.3390/min9050268
[73] Bruno, F.; Muzzupappa, M.; Barbieri, L.; Gallo, A.; Ritacco, G.; Lagudi, A.; La Russa, M. F.; Ruffolo, S. A.; Crisci, G. M.; Ricca, M.; Comite, V.; Pietraggi, B. D.; Di Stefano, G.; Guida, R. (2016). The CoMAS project: New materials and tools for improving the in situ documentation, restoration, and conservation of underwater archaeological remains. Marine Technology Society Inc. 4. 108-118. 10.4031/MTSJ.50.4.2
[74] Ruffolo S.A.; Ricca M.; Macchia A.; La Russa M.F. Antifouling coatings for underwater archaeological stone materials. Progress in Organic Coatings, Volume 104, 2017, Pages 64-71, ISSN 0300-9440, https://doi.org/10.1016/j.porgcoat.2016.12.004.
[75] Ruffolo S.A.; Macchia A.; La Russa M.F.; Mazza L.; Urzì C.; De Leo F.; Barberio M.; Crisci G.M. (2013). Marine Antifouling for Underwater Archaeological Sites: TiO2 and Ag-Doped TiO2. International Journal of Photoenergy, vol. 2013, Article ID 251647, 6 pages, 2013. https://doi.org/10.1155/2013/251647

Chapter 1

In the first chapter, the different decay phenomena affecting the Cosenza Cathedral façade (Calabria, South Italy) were assessed through the evaluation of the relative damage indices. A multidisciplinary approach was applied exploiting both NDTs and MDTs. Such a combination enabled proposing an intervention priority scale that can be helpful to institutions when planning a prompt restoration intervention. The outcomes underscore the effectiveness of this approach in establishing a comprehensive diagnostic and conservation system for Cultural Heritage. This system extends to monitoring, maintenance, and the judicious selection of restoration techniques over time, contributing to its effective management and enhancement.

This chapter has been published as:
Donato, A.; Randazzo, L.; Ricca, M.; Rovella, N.; Collina, M.; Ruggieri, N.; Dodaro, F.; Costanzo, A.; Alberghina, M.F.; Schiavone, S.; et al. Decay Assessment of Stone-Built Cultural Heritage: The Case Study of the Cosenza Cathedral Façade (South Calabria, Italy). Remote Sens. 2021, 13, 3925. https://doi.org/10.3390/rs13193925

Abstract: This study aims to assess the different decay phenomena affecting the Cosenza Cathedral façade (Calabria, South Italy) through the evaluation of the relative damage indices. For this goal, a multidisciplinary approach was applied exploiting both nondestructive and microdestructive techniques. Such a combination enabled proposing an intervention priority scale that can be helpful to institutions when planning a prompt restoration intervention. The results suggest the efficiency of this approach to obtain a multidisciplinary diagnostic and conservation system for the management and valorization of the Cultural Heritage also in terms of monitoring, maintenance, and selection of the most suitable restoration procedures over time.

Keywords: nondestructive techniques; microdestructive techniques; stone deterioration; damage indices; Cosenza; Italy

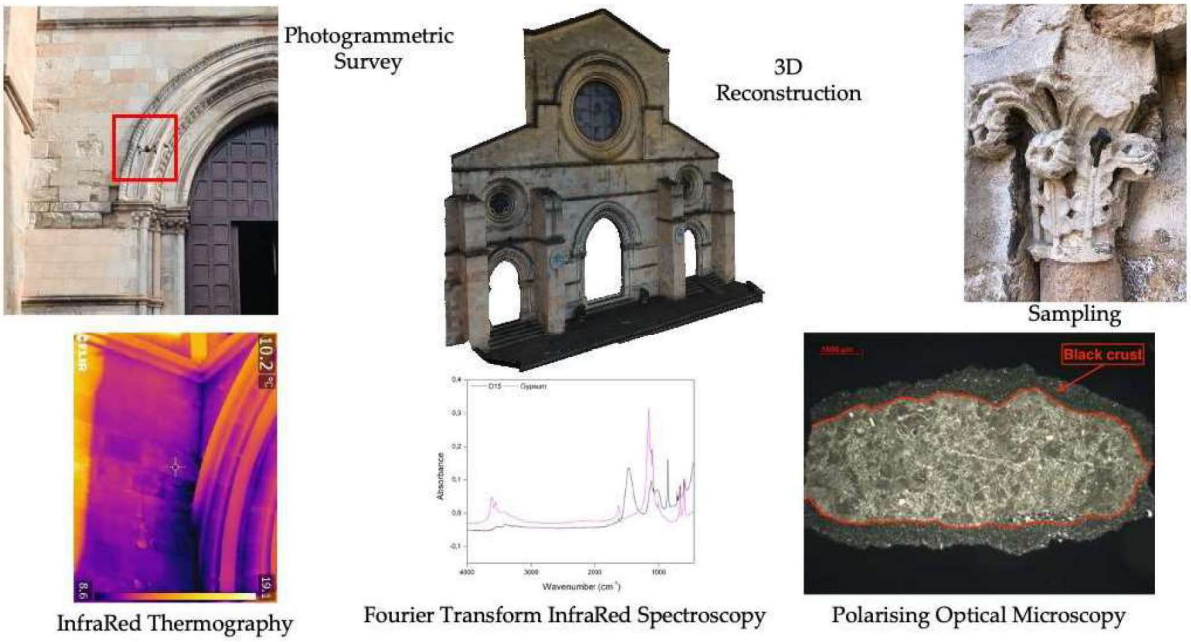

1. Introduction

The increase in weathering damage on natural stone monuments requires proper countermeasures in order to reach a sustainable monument preservation. In this regard, in recent decades, increasing attention is being paid to the multidisciplinary approach that allows a better performance of both preventive conservation and more efficient restoration action. In order to provide a proper decay assessment of stone-built heritage and the subsequent restoration plan, a single test nondestructive technique (NDT) or microdestructive technique (MDT) may not be sufficient to provide enough data; instead, a combination of different NDTs and MDTs should be performed [1–5]. Such combination can return information on stone decay from the nanoscale to mesoscale, defining a full-scale decay assessment, which would permit dictating an intervention priority list for future restoration planning. The application of both NDTs and MDTs enables defining both quantitatively and qualitatively the different decay forms encountered and the best practice for conservation and restoration interventions. Cosenza Cathedral is located in the old town of Cosenza (Calabria, southern Italy). It was originally built on Colle Pancrazio [6] and due to an earthquake on 9 June 1184, it was rebuilt under Archbishop Pietro Ruffo in the current location beginning on 9 June 1185 [7]. Its rebuilding was completed by 1222 when the cathedral, according to oral tradition, was consecrated by Emperor Frederick II. During the first half of the 18th century, the church was covered by a baroque superstructure that obliterated the original structure and its works of art. In the first half of the 19th century, the façade was transformed into neogothic style, which changed completely its original aspect. At the end of the 19th century, Archbishop Camillo Sorgente entrusted the work to Pisanti, who recovered the original old arches and the ancient structure of the church. In the 1940s, the work was finally completed [8]. On 12 October 2011, the Cathedral of Cosenza received the status of UNESCO World Heritage Site for being "Heritage Witness to a Culture of Peace". This is the first award given by UNESCO to the region of Calabria [9]. This paper aims to assess the decay phenomena affecting the Cosenza Cathedral façade and the related damage indices. The alteration and degradation forms that occurred on the façade were identified in a first nondestructive phase in situ by means of macroscopical observation and preliminary InfraRed Thermography (IRT) survey. Based on these preliminary data, several in lab analyses were carried out to characterize the different decay forms encountered both qualitatively and quantitatively, such as polarizing op-tical microscopy (POM), ion chromatography (IC), and Fourier Transform Infrared Spectroscopy (FTIR). Data collected and integrated with Photogrammetric Survey and 3D Re-construction were useful to define the damage indices of weathering forms, thus suggesting suitable restoration interventions.

2. Material and Methods

The stone mainly used for building the façade of the Cathedral, as reported in the literature [10,11], was a calcarenite, a medium-grained limestone, rather soft and easy to work. The calcarenite shows a carbonate matrix that can be defined as biocalcarenite/calcirudite or biolitite/boundstone, with rare embedded clasts of igneous and metamorphic rocks, having subangular to rounded morphology. It is a porous but resistant material with a variable chromaticity ranging from whitish to reddish hues. These variations are commonly induced by a different content of ferrous minerals although other causes cannot be excluded [12,13].

A first diagnosis in situ enabled evaluation of the distribution of the different decay phenomena affecting the façade and, consequently, the choice of the samples to be taken. Five different forms were identified, following UNI 11182 [14]: black crusts, erosion/disaggregation, efflorescences,

biological patina/superficial deposits, and loss of material. In this regard, a total of 43 samples (D1–D43) (Table 1) were taken from the façade at different heights above ground level (Figure 1).

Table 1. Brief description of samples taken with respective sampling point and analysis. Macroscopic features of investigated samples together with the sampling point according to Figure 1 and employed techniques on each sample. CLC = Fragment of calcarenite; D-CLC = Disaggregated calcarenite; EF = Efflorescences; SEF = Subefflorescences; BSL = Blackish superficial layer; GSL = Greyish superficial layer; U = Unaltered; IC = Ion Chromatography; FT-IR = Fourier transform infrared spectroscopy; POM = polarizing microscope.

Sample ID	Description	Height above Ground (m)	Employed Techniques
D1	CLC, U	1.1	IC
D2	CLC, GSL	1.1	IC
D3	CLC, GSL	2.3	POM
D4	CLC, GSL	1.4	FTIR
D5	EF	2.2	IC, FTIR
D6	D-CLC	1.8	IC
D7	CLC, U	3.0	FTIR
D8	CLC, BSL	1.6	POM
D9	CLC, U	2.6	IC, FTIR
D10	CLC, U	1.9	FTIR
D11	D-CLC, EF-SEF	2.3	IC, FTIR
D12	CLC, U	1.2	FTIR
D13	CLC, BSL	5.9	POM
D14	D-CLC, BSL	4.6	IC, FTIR
D15	D-CLC, BSL	4.8	IC, FTIR
D16	D-CLC	4.9	IC
D17	CLC, U	5.0	IC
D18	D-CLC	5.4	IC, FTIR
D19	D-CLC	5.5	IC, FTIR
D20	D-CLC, BSL	5.5	IC, FTIR
D21	CLC, BSL	7.6	POM
D22	CLC, GSL	7.3	FTIR
D23	CLC, BSL	7.5	POM
D24	CLC, BSL	7.8	FTIR
D25	CLC, BSL	8.1	FTIR
D26	CLC, GSL	9.0	FTIR
D27	CLC, U	9.2	FTIR
D28	CLC, GSL	9.3	POM
D29	CLC, U	4.3	FTIR
D30	D-CLC, BSL	4.1	FTIR
D31	CLC, BSL	4.0	POM
D32	CLC, GSL	4.0	FTIR
D33	CLC, BSL	4.1	FTIR
D34	D-CLC, BSL	7.8	IC
D35	CLC, BSL	7.2	FTIR
D36	CLC, BSL	7.7	FTIR
D37	CLC, BSL	8.2	POM
D38	CLC, BSL	8.9	POM
D39	D-CLC, BSL	7.5	IC, FTIR
D40	D-CLC, BSL	8.3	IC, FTIR

D41	CLC, BSL	15.0	FTIR
D42	CLC, GSL	14.4	FTIR
D43	CLC, BSL	22.4	POM

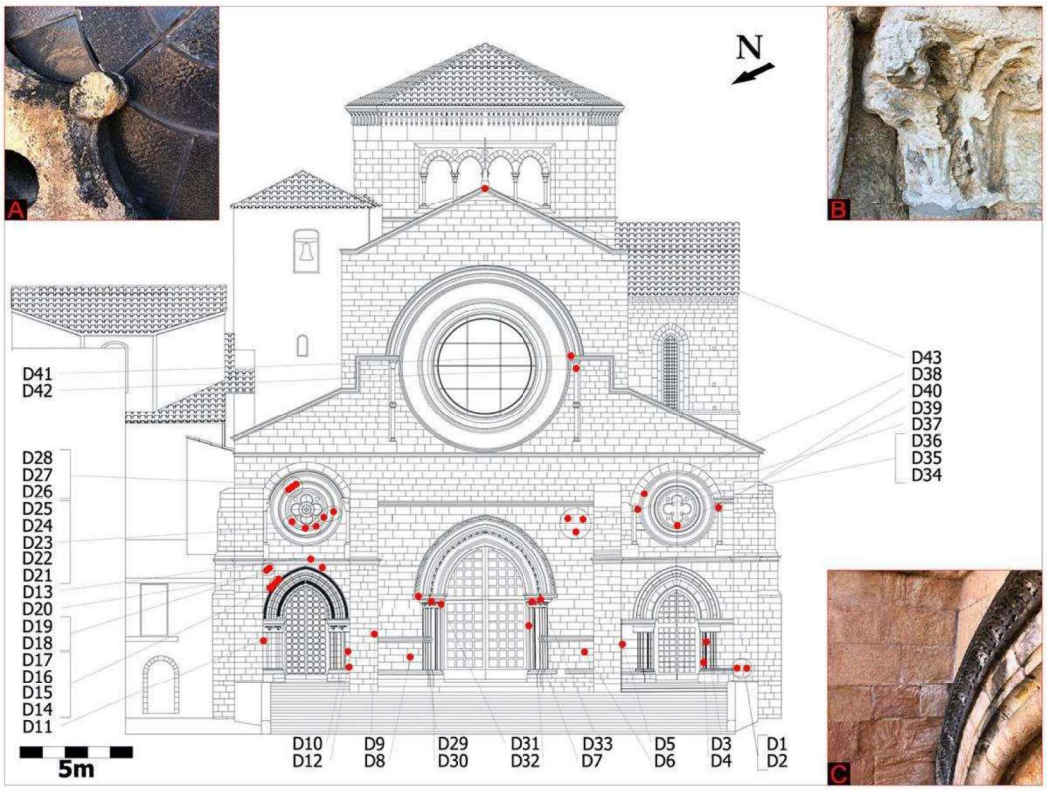

Figure 1. Samples taken from the façade. The images show some deteriorated areas in detail and relevant samples: (**A**) D21-D22; (**B**) D32-D33; and (**C**) D14-D15-D16-D17.

Next, the samples were analyzed via POM, IC and FTIR, in order to characterize qualitatively and quantitatively the different decay forms encountered. Subsequently, their detailed mapping and damage analysis were realized carrying out a photogrammetric survey (Figure 2).

Figure 2. Workflow of the process carried out.

2.1 Infrared Thermography

Infrared thermography (IRT) is a nondestructive technique widely employed in the analysis of Cultural Heritage (CH) [15,16]. In fact, IRT represents a fundamental tool in the CH diagnostic field for conservation state assessment thanks to the possibility of determining the temperature of a surface by measuring the IR radiation emitted by each object as a function of the temperature, T (°C). This technique is useful, for example, in the detection of superficial cracks, detachments, material differences, or moisture presence within structures. Indeed, the compositional or structural inhomogeneities, at or below the investigated surface, locally affect the homogeneous heat propagation and result in thermal contrast in the thermogram.

The main features investigated by the IRT technique in the monumental heritage were: (*i*) the state of conservation of architectural structures, the wall texture hidden under plaster layers, any architectural changes or additions to the original one (for example, window and door cladding); (*ii*) the quality of thermal insulation; (*iii*) the conservation state of plasters or pictorial layers, their adhesion to the support layer, the mapping of detachments or defects in the plaster, as well the identification of the different building materials due to their different emissivity value; (*iv*) moisture, water infiltrations, or dispersions, even inside the masonry whose degradation effects are not yet visible on the surface.

In the present case, a FLIR model B335 thermal imaging camera equipped with an uncooled microbolometric thermal sensor (320 × 240 pixel resolution, from −20 °C to + 120 °C thermal range, +/− 2% of the detected temperature accuracy; 7.5 ÷ 13 μm spectral range; 1.36 mrad spatial resolution; embraced field 25° × 19°) was used. The camera was also equipped with a 3.1 Mpixel photographic sensor that allowed the acquisition of the thermal image at the same time as the visible one, with the same shooting conditions.

The IRT investigation was performed without induced artificial warming of the surfaces, acquiring the data under different climatic conditions in order to take advantage of the natural heat exchange between the structure and the environment. For this reason, the thermal anomalies were documented on different days during the survey period (February and March 2021) and the temperature and relative humidity values were recorded (Table 2). Moreover, the thermographic

images were processed and calibrated also considering the specific thermohygrometric values measured at the moment of investigation.

Table 2. Temperature (T °C medium, T °C min, and T °C max) and relative humidity (RH% medium) values measured for each February and March 2021 days on which the IR thermography investigation was carried out.

Day	T °C (medium)	T °C (min)	T °C (max)	RH% (medium)
February 22	13 °C	10 °C	18 °C	76%
February 23	13 °C	7 °C	17 °C	78%
February 24	12 °C	7 °C	16 °C	83%
March 3	10 °C	4 °C	16 °C	65%
March 4	9 °C	2 °C	15 °C	81%
March 5	10 °C	2 °C	15 °C	79%

Generally, all IR thermograms could be affected by the dependence of the emissivity on the shooting angle. Then each sample area was documented through different angles, in order to guarantee the significance of the detected thermal anomalies (attributable to moisture, detachments, fractures, different materials), excluding artifacts due to the setting conditions.

2.2 Photogrammetric Survey and 3D Reconstruction

The most widespread application of photogrammetry concerns the representation of the facades or elevations of historic buildings and structure. By improving digital techniques, digital close-range photogrammetry has become a more efficient and more economic method. Obtained 3D solid or textured images help to understand sophisticated and complex buildings more easily.
One of the most important advantages of using digital close-range photogrammetry to supply documentation is in measuring dangerous or inaccessible areas, very high or low buildings, or part of these buildings. It represents an important support in obtaining the required measurement of the parts of the building from the photograph [17].

2.3 Damage Analysis

Evaluation, quantification, and rating of stone damages via monument mapping is based on objective description and registration, according to type and intensity, of weathering forms [18]. The preliminary in situ diagnosis and the photogrammetric survey enable exact location of all weathering forms affecting the façade.
While such forms are involved in the definition of deterioration phenomena according to type and intensity, damage categories and damage indices have been established as a practical tool for the rating of damage and as a contribution to risk prognosis and risk management. According to defined schemes, all weathering forms (considering different intensities) are related to damage categories [19].
Damage indices are calculated from damage categories (differentiated by area percentage; interested area over total area). Linear and progressive damage indices are defined as:

$$DI_{lin} = [(A \times 0) + (B \times 1) + (C \times 2) + (D \times 3) + (E \times 4) + (F \times 5)] \quad (1)$$

$$DI_{prog} = \sqrt{(((A \times 0^2) + (B \times 1^2) + (C \times 2^2) + (D \times 3^2) + (E \times 4^2) + (F \times 5^2))/100)} \quad (2)$$

where each letter (A–F) represents the sum of percentage area of different decay forms referred to the same damage category (0–5).

Damage indices range from 0 to 5.0. According to the defined calculation modes, the linear damage index corresponds to the average damage category, whereas the progressive damage index emphasizes proportion of the higher damage categories. The difference between those indices increases as the proportion of higher damage categories increases.

2.4 Polarizing Optical Microscopy

Polarizing optical microscopy (POM) was applied to identify the main minero-petrographic features of the stone and to characterize the superficial layers, preparing thus stratigraphic thin sections. Moreover, it was possible to obtain information about the interaction between the altered superficial layer and the substrate.
POM was performed using a Zeiss AxioLab microscope (Oberkochen, Germany) equipped with a digital camera to capture images.
Out of a total of 43 samples, 10 were selected because they were considered the most representative of the main observed degradation forms (Table 1).

2.5 Ion Chromatography and Fourier Transform Infrared Spectroscopy

The combined performance of IC and FTIR provide a quantitative and qualitative characterization of the different samples analyzed ([20] and references therein). Due to the complementarity of these two kinds of analysis, their results will be discussed together.
Ion chromatography is a method that enables determination of the concentrations of analytes in an unknown sample [21]. A Dionex DX 120 equipment on filtered supernatant (filter Minisart RC 25, diameter = 0.45 μm) provided ion-chromatography data both on untreated and treated samples, determining ionic species such as SO_4^{2-}, NO_3^-, Cl^-, F^-, Br^-, Li^+, NH_4^+, Na^+, K^+, Ca^{2+}, and Mg^{2+}.
Fourier Transform Infrared Spectroscopy (FTIR) is an analytical technique able to identify organic, polymeric, and inorganic materials. The FTIR analysis method uses infrared light to scan test samples and observe chemical properties [22].
The infrared spectra were collected with a spectrophotometer Perkin Elmer Spectrum 100 (Waltham, MA, USA), equipped with an attenuated total reflectance (ATR). The ATR accessory is equipped with a diamond crystal, in the range 500–4000 cm^{-1} at a resolution of 4 cm^{-1}.
The technique was used to analyze small amounts of black crust and/or efflorescence samples drawn from samples surfaces using a scalpel.

3. Results

3.1 Infrared Thermography

The IRT investigation was carried out on the wall structures and the architectural decorative elements of the main façade of the Cathedral, both the external and internal side.
The acquired IR thermograms made it possible:

- to map the different materials relating to the changes in the architectural system verifying the known historical information about the several restorations that the building has undergone in the past;
- to quickly assess the presence of thermal discontinuities attributable to efflorescence degradation, moisture, and physical damage on the stone surfaces of the façade.

In particular, at the lower parts of the external side, thermal anomalies associated with capillary rising phenomena were observed.
In the upper part, thermal anomalies compromising the structural proprieties and aesthetic values of the wall structures of the façade were detected. As clearly revealed in Figure 3, indeed, at the height of the lateral rose window, a wide water infiltration affects a large part of the façade.

Figure 3. Thermograms acquired on the external side (**a**) and on the corresponding internal side (**b**) and comparison with the photographic images of the same areas investigated. The colder areas (blue tones) locate the infiltration at the height of the side rose. A temperature of 12.7 °C and 64% relative humidity values measured during the 23 February 2021 in situ morning session were used to postprocess the thermograms here reported. This portion of the facade of the cathedral is related to an infiltration of rainwater from the external side of the masonry or from the roof and extends up to the frames of the rose window.

Correspondingly, on the internal side, the IRT inspection documented the higher intensity signal due to a presence of rainwater in the same portion of the wall structure. The diagnostic evidence confirmed that the rainwater infiltration through damage to the roofing system is one of the causes of the major deterioration in this wall portion.

The water migration into the porosity of the stone blocks due to evaporative phenomena led to the formation of salts efflorescence on the external side and, consequently, induced an important superficial decohesion, also identifiable in IRT images as colder surfaces.

3.2 Photogrammetric Survey and 3D Reconstruction

The 3D model can be helpful to evaluate the structures in their entirety, their conservation state and, moreover, to recognize and evaluate the distribution and the evolution of the different degradation processes characterized during the laboratory analysis. In fact, 3D imaging techniques associated with photographic documentation grant a high level of detail, making the identification of interested areas easier and more efficient as well as the assessment of damage indices.

The photogrammetric survey was carried out by a drone (Figure 4) and the subsequent data processing was realized by software as Meshlab (www.meshlab.net accessed on 15 July 2021), to generate a 3D mesh, and AutoCAD, to estimate the degraded areas.

Figure 4. Detail of photogrammetric survey.

AutoCAD software enabled association of each decay form to a single hatch; whereas the calculation of the areas was performed by AutoCAD simultaneous with the hatch creation.
The mapping of the area with individual forms of decay (previously identified), and their extensions, is reported below (Table 3, Figure 5).

Table 3. Weathering forms areas.

	Black Crusts	Erosion/ Disaggregation	Efflorescences	Biological Patina/Superficial Deposits	Loss of Material
Area (cm^2)	198,328.5	481,235.3	51,506.3	471,502.5	31,402.5
Area (%)	5.75	13.95	1.49	2.29	0.91

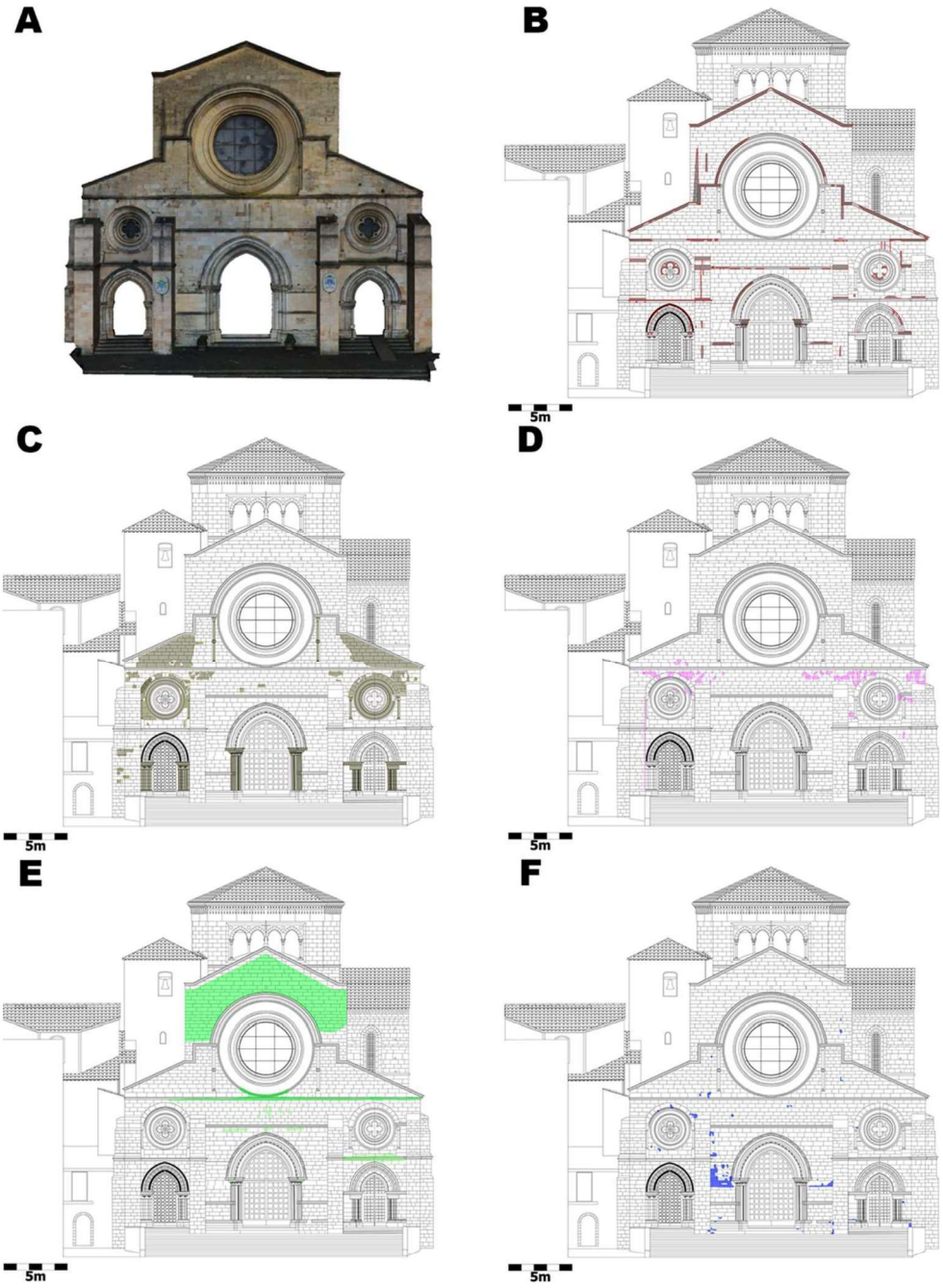

Figure 5. (**A**) 3D model of the façade; (**B**) Black crust; (**C**) Erosion/Disaggregation; (**D**) Efflorescences; (**E**) Biological patina/Superficial deposits; (**F**) Loss of material.

3.3 Damage Analysis

Damage categories were attributed to previously mentioned forms in order to calculate the linear and progressive damage indices (Table 4). Damage categories values were evaluated as an average over the whole façade.

Table 4. Damage index evaluation.

Weathering Forms		Parameters Considered during Evaluation					
Black crusts	Intensity	Cover degree of the surface (%)					
		<15	25	50	75	100	
	Damage category	0	1	2	3	4	5
Erosion/ Disaggregation		Depth (mm and/or cm)					
	Intensity	<0.5	0.5–1	1–3	3–5	5–10	10–25
	Damage category	0	1	2	3	4	5
Efflorescences		Cover degree of the surface (%)–Color change degree					
	Intensity	<10	25	50	75	100	
		Chromatic alteration		Whitening			
	Damage category	0	1	2	3	4	5
Biological patina/ Superficial deposits		Cover degree of the surface (%)					
	Intensity	<10	25	50	75	100	
	Damage category	0	1	2	3	4	5
Loss of material		Cover degree of the surface (%)					
	Intensity	<10	25	50	75	100	
	Damage category	0	1	2	3	4	5

Damage indices obtained for the entire façade were equal to:

$$DI_{lin} = 0.86 \quad (3)$$

$$DI_{prog} = 1.66 \quad (4)$$

The difference between progressive and linear indices is an indication of how much the decay forms belonging to higher damage category (efflorescences and erosion in this case) weigh on the indices' calculations.

As highlighted during in situ decay observations, the left side of the façade was mostly affected by both efflorescences and erosion phenomena; therefore, damage indices were determined also on the two portions of the façade (left and right). The damage indices of the two portions were respectively: DI_{lin} = 1.06 and DI_{prog} = 2.06 for the left side, DI_{lin} = 0.67 and DI_{prog} = 1.27 for the right side. They suggest the necessity to intervene urgently in this area with a restoration plan.

3.4 Polarizing Optical Microscopy

Petrographic observations suggest how all samples show similar features; in particular, they can be classified as biosparites/biopelsparites (Folk classification [23]) or wackestone (Dunham classification [24]). The most abundant accessory clasts were mostly siliciclastics, as quartz, plagioclase, micas (biotite, muscovite), and polycrystalline quartz. Fragments of granitoid rocks were found in D13 and D21 thin sections (Figure 6).

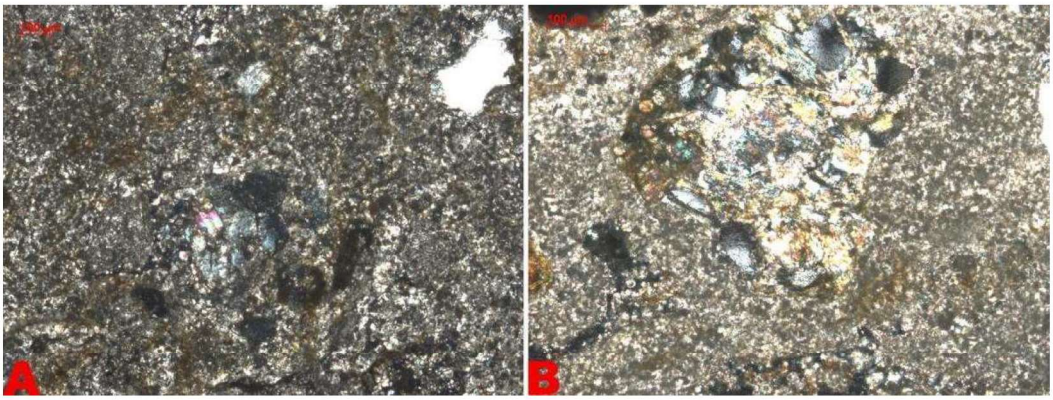

Figure 6. Fragments of granitoid in D13 (**A**) and D21 (**B**) samples (crossed polarized light view, CPL).

The samples appear to be compact, with the exception of D21, D23, D28, and D31 where a slight fracturation was detected, with a secondary porosity <20%.

A superficial layer with variable thickness, made of microcrystalline gypsum, was observed on D13, D23, D31, D37, and D43 specimens. The level was related to the degradation forms (black crusts) identified under macroscopic observation. Traces of *scialbatura* (i.e. a sort of thin finishing lime layer) were found in D28 and D38 thin sections (Figure 7A, B).

The superficial layer was discontinuous in most of the samples, with an average thickness ranging from 120 μm to 265 μm. It showed an irregular lower profile, while the upper one varied from irregular to lobate (Figure 7C, D). D37 was the only sample in which the superficial layer showed different characteristics. It appeared to continue in the whole sample, with a thickness ranging from 350 to 900 μm. The crust was adherent to the substrate, except in some parts where it was fractured. The superficial layer was constituted mainly of microcrystalline gypsum; in addition, it was possible to observe also acicular gypsum crystals, Fe-oxides, and carbonaceous particles (Figure 7E, F).

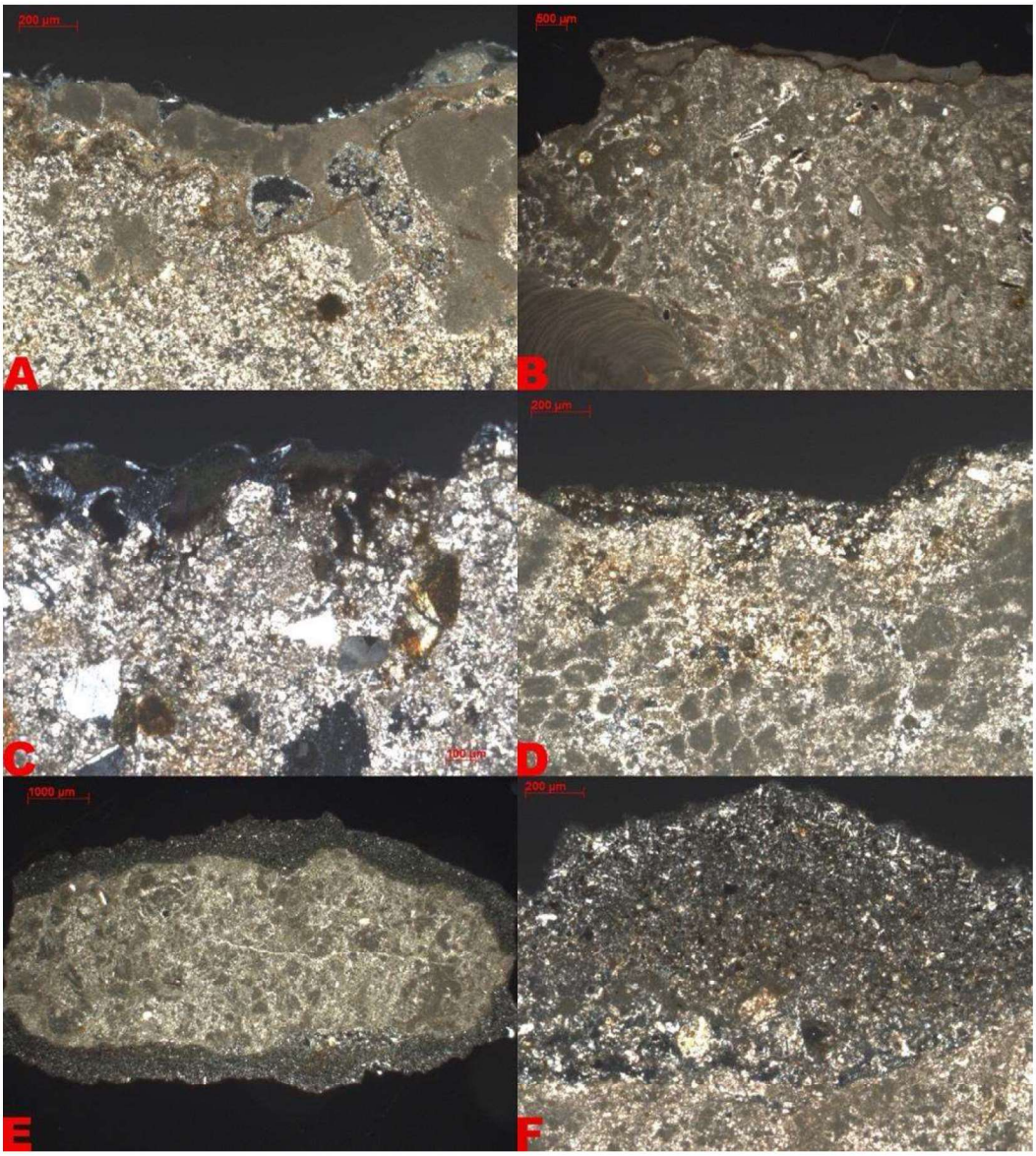

Figure 7. (**A**,**B**) *Scialbatura* traces in D28 and D38 thin sections; (**C**) Siliciclastic accessory clasts mainly encountered; (**D**) Superficial layer overlying the substrate in D31 sample; (**E**,**F**) D37 sample and detail of the overlying black crust with visible acicular crystals of gypsum, Fe-oxides, and carbonaceous particles.

3.4 Ion Chromatography and Fourier Transform Infrared Spectroscopy

IC analysis showed most of the samples were characterized by a high amount of sulphate and carbonate, associated with sodium and calcium (Table 5, Figure 8).

Table 5. Anions and cations concentrations (mg/L).

Sample ID	Li^+	Na^+	NH_4^+	K^+	Mg^{2+}	Ca^{2+}	Sr^{2+}	F^-	Cl^-	HCO_3^-	Br^-	NO_3^-	PO_4^{3-}	SO_4^{2-}
D1	0.0	3.4	0.1	1.4	2.5	10.3	0.2	0.3	2.0	19.8	0.0	2.8	0.0	12.7
D2	0.0	3.4	0.0	2.5	1.8	29.1	0.0	0.2	1.5	21.4	0.0	9.6	0.0	62.4
D5	0.0	106.1	0.0	17.0	0.2	1.8	0.0	0.1	2.7	230.3	0.0	23.0	0.0	74.4
D6	0.0	2.9	0.0	1.0	1.6	6.7	0.0	0.0	2.2	25.9	0.0	6.7	0.0	3.9
D9	0.0	3.6	0.1	1.1	2.1	35.8	0.0	0.1	2.5	16.8	0.0	4.4	0.0	81.0
D11	0.0	53.2	0.0	0.8	0.4	1.6	0.0	0.2	0.5	172.4	0.0	0.9	0.5	20.0

D14	0.0	2.5	0.0	0.3	1.3	107.3	0.6	0.1	0.6	18.3	0.0	1.5	0.0	289.3
D15	0.0	1.8	0.2	0.3	1.5	144.0	1.4	0.5	0.3	29.0	0.0	0.3	0.0	308.3
D16	0.0	0.7	0.1	0.3	1.9	7.0	0.0	0.4	0.3	32.0	0.0	0.2	0.0	5.2
D17	0.0	2.3	0.0	0.4	1.8	5.8	0.0	0.1	0.2	36.6	0.0	0.3	0.0	1.7
D18	0.0	56.7	0.0	1.1	0.6	2.6	0.0	0.1	0.9	152.5	0.0	2.6	0.0	17.4
D19	0.0	47.0	0.0	1.0	0.5	2.3	0.0	0.1	2.2	128.1	0.0	6.4	0.0	14.4
D20	0.0	2.7	0.1	0.6	2.1	58.6	0.0	0.1	2.4	45.8	0.0	2.0	0.0	131.6
D34	0.0	2.1	0.2	0.6	6.2	11.3	0.0	0.5	1.3	67.1	0.0	5.1	0.0	6.6
D39	0.0	1.2	0.1	0.4	1.3	86.7	0.9	1.2	0.8	38.1	0.0	1.6	0.0	224.8
D40	0.0	1.3	0.0	0.4	1.9	74.7	0.0	0.3	0.9	42.7	0.0	0.6	0.0	182.3

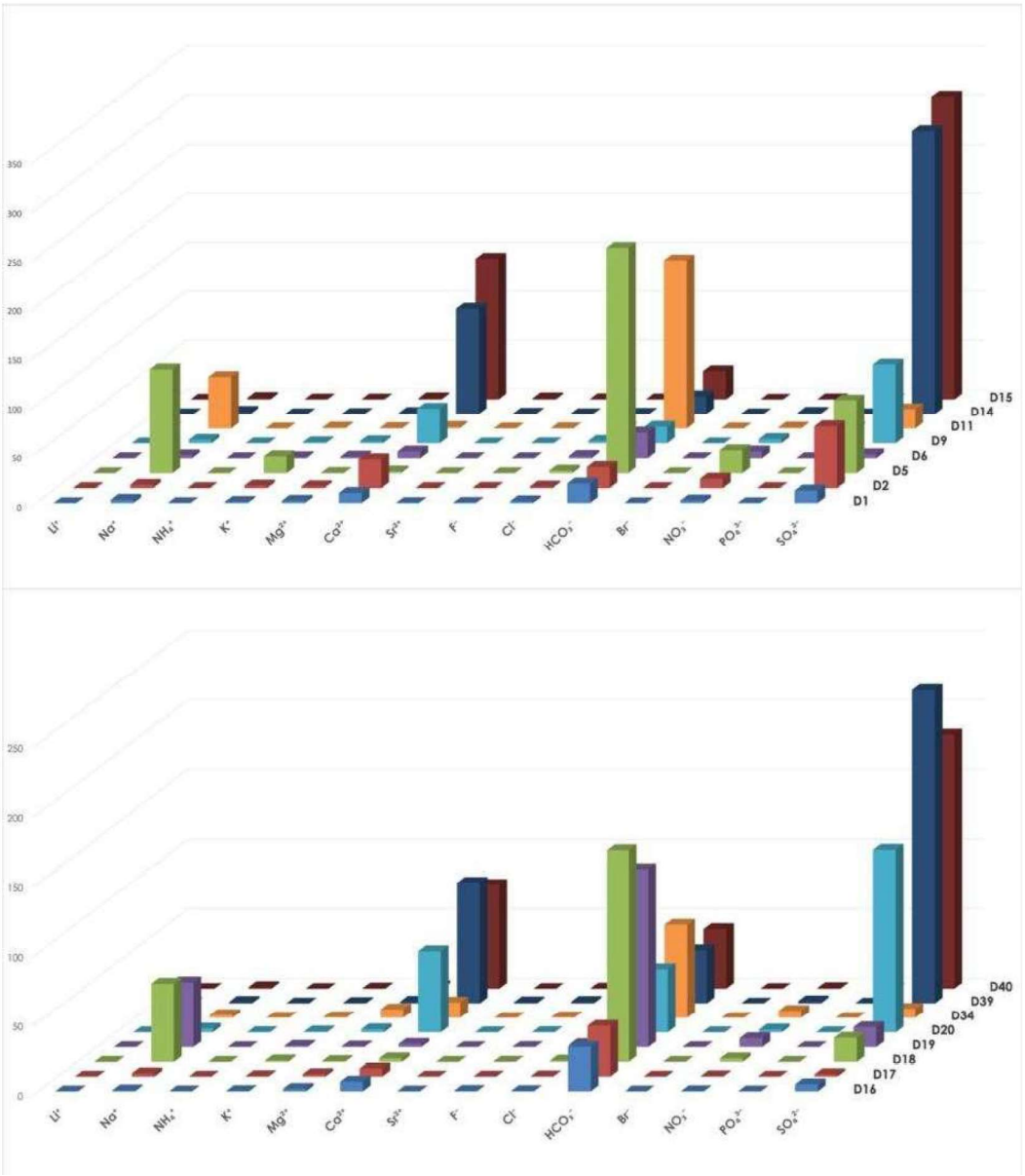

Figure 8. Anion and cation concentrations (mg/L).

From the study of vibrational bands via FTIR, many mineralogical phases were identified, such as gypsum and calcite (Figure 9); moreover, traces of silicates were found (Table 6).

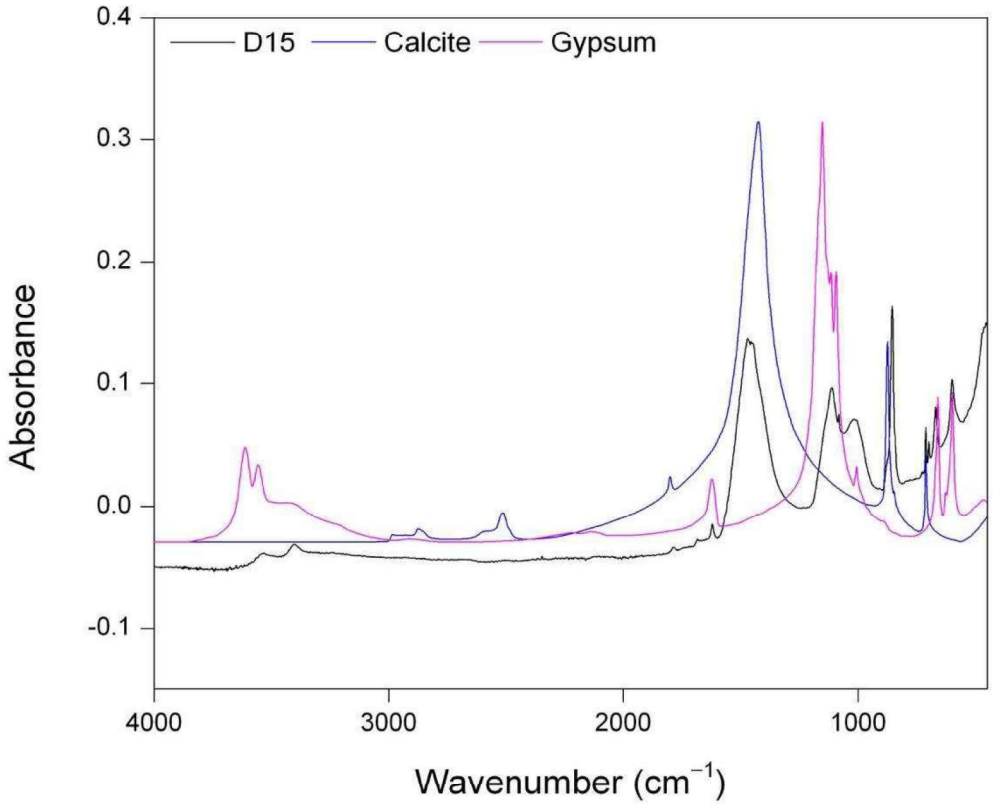

Figure 9. D15 sample IR spectra.

Table 6. Vibrational bands (wavenumber cm^{-1}) of the different mineralogical phases identified.

Sample ID	Calcite	Gypsum	Silicates
D4	1429, 879, 729		1646, 1167, 1082, 781
D7	1429, 877, 729		1646, 1085, 781
D9	1440, 878, 729	3546, 3403, 1621, 671, 609	1679, 1140, 1119
D10	1434, 877, 727		1022, 1084, 781
D11	1404, 875, 713		1661, 1082, 1016
D12	1435, 877, 727	3551, 3410, 1621, 661, 600	1623, 1082, 1038
D14	1458, 856, 713	3541, 1622, 1109, 1009, 670, 596	
D15	1779, 1447, 855, 714	3531, 3407, 1621, 1113, 1084, 1010, 670, 601	
D18	1403, 874, 713	3453, 1654, 648, 615	1790, 1082, 692
D19	104, 873, 714	3351, 1656, 649, 614	1790, 1081, 693
D20	1787, 1447, 874, 713	3542, 1622,1116, 1084, 670, 601	1083, 782, 700
D22	1804, 1435, 878, 730		1652, 1080, 1031, 781
D24	1788, 1427, 878, 729		1640, 1083, 1031, 783
D27	1808, 1417, 876, 728		1645, 1031, 784, 665
D29	1800, 1417, 873,7 13	3554, 1621, 1121, 669, 602	1667, 1083, 783
D30	1791, 1415, 875, 713	3410, 1641, 607	1788, 1082, 698
D35	1793, 1417, 874, 713		1647, 1008

D39	1787, 1446, 855, 713	3542, 1621, 1116, 1093, 670, 600	
D40	1785, 1446, 879, 710	3541, 3400, 1621, 1112, 1082, 671, 607	

The presence of calcite can be attributed to the carbonate substrate while the presence of gypsum may depend on sulfation reactions caused by polluting agents, associated with black crust and efflorescence genesis.
The IC results showed a good correlation between calcium and sulphate, testifying, according to FTIR analysis, that these two species were mainly present in the form of gypsum. The same behavior could not be determined for sodium and chlorine. In fact, an excess of sodium was evident in all samples compared to chlorine. This may be due to the presence of sodium sulphates as well as sodium chloride. As is well known, the presence and the crystallization of these soluble salts from repeated cycles of crystallization/dissolution within the porous matrix of the stone in porous materials is one of the major causes of rock decay in nature [25] and weathering of natural and/or artificial building material [26–28]. The growth of a crystal in a confined space (pore) can alter both the porosity and the pore size distribution of the stones, changing also their mechanical properties [29]. This process is emphasized in some sulphate species, particularly sodium sulphate. It exerts crystallization pressures on the pore walls, and in addition, undergoes a change in volume during its transition to the hydrated form (mirabilite), producing also a certain hydration pressure. The data collected in Table 4, report the largest concentration of these sodium sulphates in D5, D11, D18, and D19 coming from the portion of the church façade where efflorescences were much more intense. These samples also showed the highest rate of disintegration and fracturing, confirming the damaging effect of salt crystallization.

4. Discussion

The use of nondestructive techniques such as IRT and photogrammetric survey provided helpful data to define the areas of major interest that needed further investigation and to be sampled. The results of the temperature behavior of the stone materials can contribute to the characterization of stone types, weathering state and damage, and exposition settings. Moreover, such results can also indicate areas which are affected by high humidity load (e.g., façade left part).
The combination of those techniques was crucial in terms of efficiency and time-consuming analysis as both techniques are quite quick to execute. Reducing time for diagnosis enables producing a faster response for institutions when planning a prompt restoration intervention.
Following a priority scale provided by damage categories assigned to different weathering forms, it would be recommendable to intervene firstly on areas affected by efflorescences, paying attention to the area above the left portal of the façade; while erosion covers about 14% of the façade, efflorescences may exacerbate the strong erosion already present and the combined effect of those may compromise the conservation of the whole structure. Although the area above the right portal of the façade has efflorescences, they are less intense; the uneven progression between these parts could be due to a heavy water infiltration on the left part, as highlighted by IRT, which favored its evolution over time. Finally, a cleaning intervention is required on areas affected by black crusts and biological patina.

5. Conclusions

The diagnostic phase carried out in situ combined with the results of in lab analysis and the integration with the 3D model demonstrated the efficiency of this multidisciplinary approach in the assessment of the conservation state of built heritage and in the planning of the restoration interventions.

Nondestructive techniques enabled characterization of the damage on the façade on a mesoscale, while microdestructive techniques from nano to microscale, provided a complete decay assessment of the case study and the subsequent intervention priority scale.

This survey may represent a good practice to develop a damage diagnosis, leading to important practical concerns for an acceptable decision-making process to be applied in future restoration of stone-built heritage. In this regard, the results will be later integrated into an information system, available in realtime, allowing institutions to monitor its conservative status over time.

References

1. Diz-Mellado, E.; Mascort-Albea, E.J.; Romero-Hernández, R.; Galán-Marín, C.; Rivera-Gómez, C.; Ruiz-Jaramillo, J.; Jaramillo-Morilla, A. Non-destructive testing and Finite Element Method integrated procedure for heritage diagnosis: The Seville Cathedral case study. *J. Build. Eng.* **2021**, *37*, 102134, https://doi.org/10.1016/j.jobe.2020.102134.
2. Chastre, C.; Ludovico-Marques, M. Chapter 13—Nondestructive testing methodology to assess the conservation of historic stone buildings and monuments. In *Handbook of Materials Failure Analysis*; Makhlouf, A.S.H., Aliofkhazraei, M., Eds.; Butterworth-Heinemann: Oxford, UK, 2018; pp. 255–294, https://doi.org/10.1016/B978-0-08-101928-3.00013-6.
3. Kilic, G. Using advanced NDT for historic buildings: Towards an integrated multidisciplinary health assessment strategy. *J. Cult. Herit.* **2015**, *16*, 526–535, https://doi.org/10.1016/j.culher.2014.09.010.
4. Bosiljkov, V.; Uranjek, M.; Žarnić, R.; Bokan-Bosiljkov, V. An integrated diagnostic approach for the assessment of historic masonry structures. *J. Cult. Herit.* **2010**, *11*, 239–249, https://doi.org/10.1016/j.culher.2009.11.007.
5. Bosiljkov, V.; Maierhofer, C.; Koepp, C.; Wöstmann, J. Assessment of Structure through Non-Destructive Tests (NDT) and Minor Destructive Tests (MDT) Investigation: Case Study of the Church at Carthusian Monastery at Žiče (SLOVENIA). *Int. J. Archit. Herit.* **2010**, *4*, 1–15, doi:10.1080/15583050902731031.
6. Andreotti, D. *Storia dei Cosentini*, 1st ed.; Pellegrini: Cosenza, Italy, 1978; Volume 1.
7. Rubino, G.E.; Teti, M.A. *Cosenza. Le Città Nella Storia d'Italia*, 1st ed.; Laterza, Roma, Italy, 1997.
8. Mascioni Organs. Available online: https://www.mascioni-organs.com/en/cosenza-italy-cathedral/ (accessed on 15 July 2021).
9. Your Italy. Available online: https://www.youritaly.it/en/guides/calabria/the-city-of-cosenza (accessed on 15 July 2021).
10. Crisci, G.M.; De Francesco, A.M.; Gattuso, C.; Miriello, D. Un metodo geochimico per la determinazione della provenienza di lapidei macroscopicamente omogenei. Un esempio di applicazione sui monumenti del centro storico di Cosenza. *Arkos Sci. Restaur. Archit.* **2012**, *2*, 52–59.
11. Mastrandrea, A.; Muto, F.; Neri, C.; Papazzoni, C.A.; Perri, E.; Russo, F. Deep-Water Coral Banks: An Example from the "Calcare di Mendicino" (Upper Miocene, Nothern Calabria, Italy). *Facies* **2012**, *47*, 27–42.
12. Randazzo, L.; Collina, M.; Ricca, M.; Barbieri, L.; Bruno, F.; Arcudi, A.; La Russa, M. Damage Indices and Photogrammetry for Decay Assessment of Stone-Built Cultural Heritage: The Case Study of the San Domenico Church Main Entrance Portal (South Calabria, Italy). *Sustainability* **2020**, *12*. 5198.
13. Ricca, M.; Le Pera, E.; Licchelli, M.; Macchia, A.; Malagodi, M.; Randazzo, L.; Rovella, N.; Ruffolo, S.; Weththimuni, M.; La Russa, M. The CRATI Project: New Insights on the Consolidation of Salt Weathered Stone and the Case Study of San Domenico Church in Cosenza (South Calabria, Italy). *Coatings* **2019**, *9*, 330.
14. UNI 11182. Cultural Heritage. Natural and Artificial Stone. Description of the Alteration—Terminology and Definition; Ente Nazionale Italiano di Unificazione (UNI): Milan, Italy, 2006.

15. Mercuri, F.; Cicero, C.; Orazi, N.; Paoloni, S.; Marinelli, M.; Zammit, U. Infrared Thermography Applied to the Study of Cultural Heritage. *Int. J. Thermophys.* **2015**, *36*, 1189–1194, https://doi.org/10.1007/s10765-014-1645-x.
16. Moropoulou, A.; Avdelidis, N.P.; Karoglou, M.; Delegou, E.T.; Alexakis, E.; Keramidas, V. Multispectral Applications of Infrared Thermography in the Diagnosis and Protection of Built Cultural Heritage. *Appl. Sci.* **2018**, *8*, 284, https://doi.org/10.3390/app8020284.
17. Yilmaz, H.M.; Yakar, M.; Gulec, S.A.; Dulgerler, O.N. Importance of digital close-range photogrammetry in documentation of cultural heritage. *J. Cult. Herit.* **2007**, *8*, 428–433.
18. Fitzner, B.; Heinrichs, K. Damage diagnosis at stone monuments—Weathering forms, damage categories and damage indices. *Underst. Manag. Stone Decay*. **2001**, *45*, 1–49.
19. Fitzner, B.; Hinrichs, K.; La Bouchardiere, D. Damage Index for Stone Monuments. In *Protection and Conservation of the Cultural Heritage of the Mediterranean Cities, Proceedings of the 5th International Symposium on the Conservation of Monuments in the Mediterranean Basin, Sevilla, Spain, 5–8 April 2000*; Swets, Zeitlinger: Lisse, The Netherlands, 2000.
20. Montana, G.; Randazzo, L.; Mazzoleni, P. Natural and anthropogenic sources of total suspended particulate and their contribution to the formation of black crusts on building stone materials of Catania (Sicily). *Environ. Earth Sci.* **2012**, *67*, 1097–1110, https://doi.org/10.1007/s12665-012-1554-x.
21. OSU Chemistry REEL Program. Available online: https://research.cbc.osu.edu/reel/research-modules/environmental-chemistry/instrumentation/instrument-calibration/ion-chromatography-theory/ (accessed on 15 July 2021).
22. RTI Laboratories. Available online: https://rtilab.com/techniques/ftir-analysis/ (accessed on 15 July 2021).
23. Folk, R.L. Spectral subdivision of limestone types. *Bull. Am. Assoc. Pet. Geol.* **1962**, *1*, 62–84.
24. Dunham, R.J. Classification of Carbonate Rocks According to Depositional Textures. *Amer. Ass. Pet. Geol.* **1962**, 108–121.
25. Evans, I.S. Salt crystallization and rock weathering: A review. *Rev. Géomorphol. Dyn.* **1970**, *19*, 153–177.
26. Winkler, E.M. *Stone in Architectur*, 1st ed.; Springer: Berlin/Heidelberg, Germany, 1994.
27. Goudie, A.S.; Viles, H.A. *Salt Weathering Hazard*, 1st ed.; Wiley: London, UK, 1997.
28. Rodriguez-Navarro, C.; Doehne, E. Salt weathering: Influence of evaporation rate, supersaturation and crystallization pattern. *Earth Surf. Process. Landf.* **1999**, *24*,191–209.
29. Dei, L.M.; Mauro, M.; Baglioni, P.; Del Fa, C.M.; Fratini, F. Growth of crystal phases in porous media. *Langmuir* **1999**, *15*, 8915–8922.

Chapter 2

In the second chapter, the same multidisciplinary approach was employed for the first time to study the stone materials, wall paintings and related degradation forms in the Cathedral of Gerace. It allowed to characterize and preliminarily evaluate the state of conservation of the Gerace Cathedral building materials, providing useful data for the planning of future restoration interventions. In fact, in the context of scientific research conducted on Cultural Heritage, the approach represents a necessary prerequisite for planning the best restoration and protection plan possible, as already highlighted in the first chapter.

This chapter has been published as:
M. Ricca, **A. Donato**, M. Cirone, S.A. Ruffolo, A. Costanzo, M.F. Buongiorno, G. Mantella, M. F. La Russa, L. Randazzo, Building materials and decay assessment of the Gerace Cathedral (Reggio Calabria, Southern Italy); Case Studies in Construction Materials, Volume 19, 2023, e02225; ISSN 2214-5095; https://doi.org/10.1016/j.cscm.2023.e02225

Abstract: A multi-analytical approach was employed for the first time to study the stone materials, wall paintings and related degradation forms in the Cathedral of Gerace (Reggio Calabria, southern Italy). With an area of around 1898 square meters, the Gerace Cathedral is the largest in Calabria: its construction dates back to the Norman era (between 1085 and 1120), and currently displays distinct features of Greek and Latin architectural orders.
Despite having undergone numerous restorations, the church perfectly preserves its original buildings materials. Following an extensive site inspection campaign, supported by the experts dealing with building restoration, several areas were selected for analyses. Both in situ investigations and laboratory tests were carried out on micro-fragments using Non-Destructive and Micro-Destructive Techniques (NDTs and MDTs). The first step involved an inspection through InfraRed Thermography (IRT) in order to map the internal walls of the Cathedral and identify zones with potential degradation phenomena. Subsequently, a more in-depth study was designed based on the thermographic results, and laboratory tests were carried out on micro-fragments and powders to characterize the different kinds of materials (i.e., stones, mortars, plasters and pigments) and decay agents (i.e., salts and efflorescences). Thirty-one samples were subjected to a complementary analytical approach which included Polarizing Optical Microscopy (POM), Ion Chromatography (IC), X-Ray Powder Diffraction (XRPD) and Scanning Electron Microscopy (SEM) coupled with microanalysis (EDS).
The results allowed us to preliminarily characterize the different materials from which the Cathedral was built, determine its state of conservation and provide a better knowledge of the entire building, revealing details not visible to the naked eye which are important for future conservation interventions. As for the state of conservation, the integrated use of various techniques enabled the detection of rising damp generally correlated with the occurrence of water infiltration and migration phenomena which appear to affect a large part of the building, causing noticeable damage (i.e., loss of surface material, micro-cracks, white salt efflorescence, etc.). The characterization of the materials carried out on mortars, plasters, and pigments also confirmed the local origin of the raw materials. However, the provenance of the studied marbles and crystalline limestones, could not be established and, therefore, further in-depth studies are required.

Keywords: Diagnostic, Gerace Cathedral, Stone Materials, Pigments, Plasters, Restoration

1. Introduction and historical background

The degradation of cultural heritage materials represents one of the most prominent threats to their preservation. During their useful life, materials are commonly subjected to degradation processes through their exposure to specific environmental conditions as well as chemical, physical, and biological phenomena. Hence, ageing is a critical factor in the durability and use of building materials which can lead to irreversible losses if not addressed in time [1-6]. In such a context, the scientific community generally encourages interdisciplinary research to implement new conservation and protection strategies for preserving cultural heritage. Current research [1-6] illustrates that in order to study the decay of building materials and perform effective restoration interventions, a cohesive, holistic, and multidisciplinary approach is needed which includes the historical, archaeological, and architectural documentation, environmental monitoring, and evaluation and characterization of materials, as well as a knowledge of any previous interventions. To achieve this goal, the scientific community can use both Non-Destructive (NDTs) and Micro-Destructive Techniques (MDTs) which are useful for the characterization of building materials and the determination of the pathologies affecting a monument [1, 2].

This paper presents the case study of the Cathedral of Gerace (Italy). The study deals with the decay affecting some building materials and provide an in-depth scientific survey performed to understand and demonstrate the causes of deterioration.

The Cathedral of Gerace, dedicated to Santa Maria Assunta (Figure 1), was probably built between the second half of the penultimate decade of the 11th century and the first years of the 12th century on the remains of a pre-existing sacred building devoted to Aghìa Kyriakì (Saint Ciriaca) dating back to 7th-8th century [7]. It was then completed around the 4th decade of the 12th century under the Normans rule [8-9]. Due to numerous earthquakes which strongly damaged the historic center of Gerace, such as that of central Calabria in 1659 [10] or the Calabrian seismic sequence of 1783 [11], the building underwent various modifications and renovations over the centuries, while retaining its original structure, characterized by a simplicity of the longitudinal body in contrast with the complex articulation of the presbytery [7]. The structure is built from local stone, a light beige-grayish limestone, devoid of redundant embellishments and with rigorous shapes closely linked to the aesthetic-stylistic traits of the Normans [8]. The complex is visibly divided into two overlapping parts dating back to different periods: the underground Crypt and the upper church (the main basilica), the latter with a transept apse to the east and a main entrance to the west. The facade is not entirely visible from the outside, due to the adjacent buildings and especially the bell tower which hides the view of its width [7]. The front is tripartite (with three compartments), Romanesque, and has only very slight pilasters, hanging arches, and elegant splays at the openings [12-14].

The basilica-type church with a large protruding transept has a Latin cross and three naves, separated by two rows of ten columns each in granite and marble, on which stand round arches consisting of local stone and surmounted by as many capitals [7]. The lower part of the Cathedral, the Crypt, can be descended into from the left transept, through seventeenth-century internal stairs [15].

The Crypt is the oldest section of the Cathedral, probably built on a Byzantine rock church [7]. In its current configuration, the Crypt resembles an aggregate of small cross vaults supported by twenty-six slender columns of very different quality and sizes [16]. This area is characterized by a longitudinal arm deriving from a large pre-existing Byzantine oratory, and by a transverse arm, which corresponds to the upper transept of the Cathedral with which it is contemporary [15]. In the Crypt, the Sacello della Madonna dell'Itria, which is carved into the rock, is closed by a seventeenth-century wrought iron gate installed by the workers of Serra S. Bruno [7].

Leaving the Crypt, two of the three semi-circular apses dominate the Piazza della Tribuna and protrude from an imposing limestone wall. These, placed on the same line, are slightly asymmetrical due to seismic events which have been invalidating the structure since the Swabian era [7].
The Cathedral of Maria Assunta of Gerace, despite numerous alterations and restorations, remains the most imposing Norman building in Calabria [17], and has also been declared Architectural Heritage of National Interest. In 1996, following an agreement between the Diocese of Gerace, the Municipality, and the Superintendence, a large intervention was proposed which envisaged, in addition to the restoration and consolidation of the structures of the entire extended citadel, its re-functionalization [18].
In recent decades, the structure has displayed areas with a poor state of conservation, which the present study aims to investigate. Specifically, the study was carried out in two phases: a diagnostic stage conducted on-site, and an analytical one, conducted in the laboratory. In particular, the on-site diagnosis phase made it possible allowed us to perform a preliminarily identification and evaluation of the intensity of the degradation forms and to choose the most suitable sampling areas for a more in-depth study. The on-site diagnosis was carried out by means of visual inspections and InfraRed Thermography (IRT). The latter is a non-destructive technique that is widely employed in the analysis of Cultural Heritage [19, 20] as it allows the determination of the temperature of a surface by measuring the IR radiation emitted by each object as a function of the temperature, T (°C). This feature has a use in numerous different applications [21]; for example, IRT technique is widely used in building inspection to detect superficial cracks, detachments, different types of materials, or the presence of moisture within structures [22, 23]. The temperature distribution on the surface of artefacts, facades, and walls provides very useful information for discovering hidden materials and specific conditions related to their thermal performance, which may also depend on the state of conservation and maintenance interventions [23, 24].
Moreover, different kinds of materials (i.e., stones, mortars, plasters and pigments) as well as decay agents (i.e., salt efflorescences) were investigated. The samples were subjected to a complementary analytical approach, specifically involving Polarizing Optical Microscopy (POM), Ion Chromatography (IC), X-Ray Powder Diffraction (XRPD), and Scanning Electron Microscopy coupled with electron-dispersive X-ray spectroscopy (SEM-EDS). The analytical phase allowed us to characterize the stone samples, raw materials, and their degradation forms, and to define the main composition of the pictorial films (i.e., pigmenting compounds/pictorial layers).

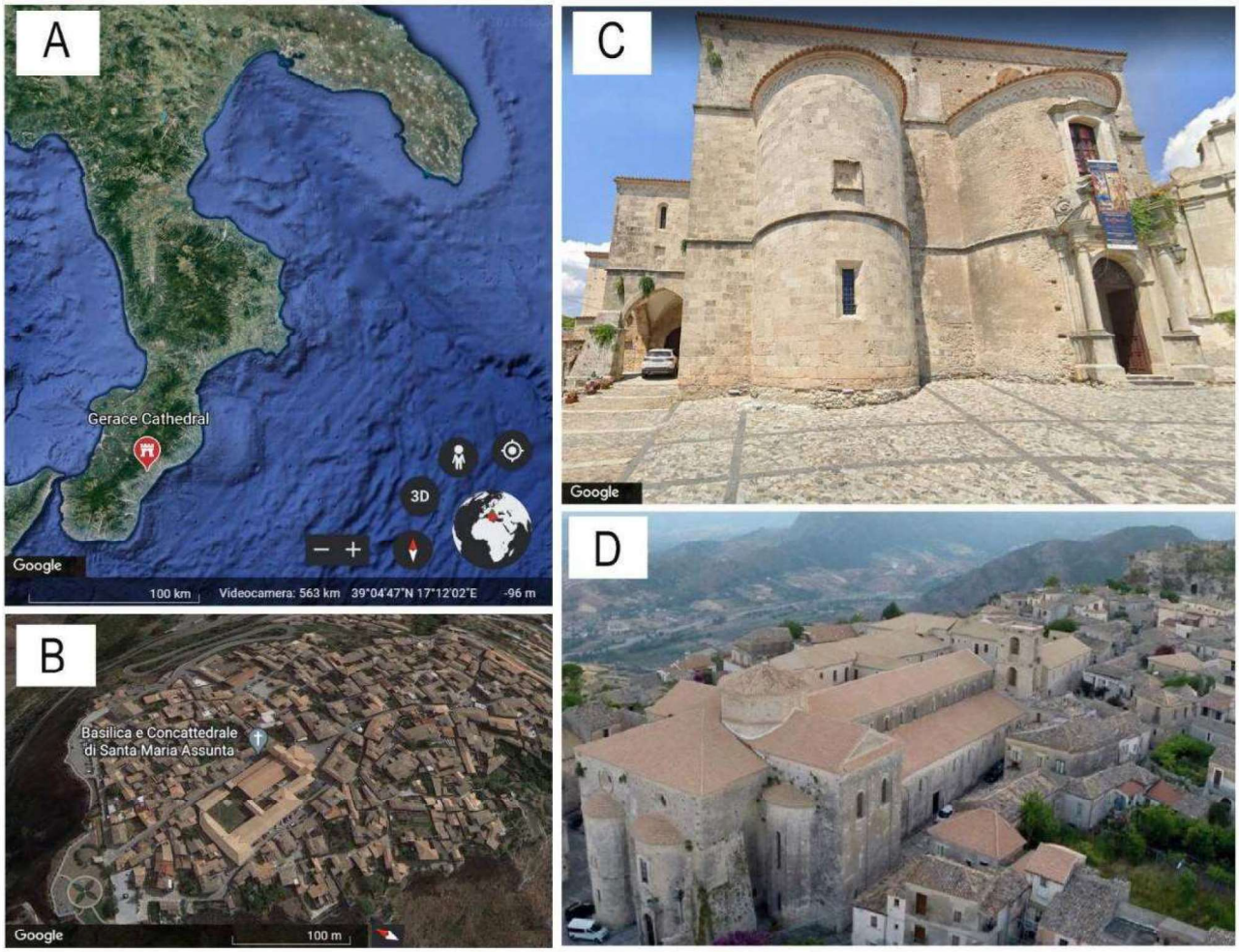

Figure 1. Location of Gerace in the Calabria region (Italy) (A) and aerial view of the Cathedral within the town (B); Front (C) and panoramic (D) views of the monument. Note: the images were obtained from Google Earth and calabriatours.org

2. Analytical methods and sampling

The main purpose of this preliminary diagnostic study was to characterize the main materials and detect any forms of degradation and related causes, in order to provide the necessary information for a future restoration project in areas of the Cathedral suffering from a serious state of deterioration. To this end, the adopted methodological approach involved: a) choosing the study areas of the Cathedral following the requests of experts and restorers in charge of the building maintenance; b) an in-situ inspection and evaluation of selected areas to be examined; c) an investigation by IRT and micro-destructive techniques following a micro-sampling campaign. In particular, the inspection of some internal wall surfaces with in-situ methods has proved to be very effective, minimizing contact with already visibly altered surfaces and facilitating the assessment of the state of conservation of the historical building. For the laboratory investigations, thirty-one samples, including both micro-fragments and powders, were sampled from areas with already existing lacunae and alterations. It is worth underlining that the sampling procedure was conducted according to principles of minimal invasiveness, collecting representative samples. Details on the sampling areas are summarized in Figs. 2 and 3, while all the analytical techniques employed and sampling campaign are described below and further summarized in Table 1.

2.1 InfraRed Thermography

In this study, IRT was used to map the surface temperatures, thus revealing the presence of thermal anomalies arising from decay processes affecting the Cathedral as a whole. It is worth noting that particular attention was paid during this phase to investigating the internal walls, in the vicinity of the areas under restoration. The survey was carried out with a FLIR model B335 thermal imaging camera equipped with an uncooled microbolometer (320 ×240-pixel resolution, over a − 20 ◦C to + 120 ◦C thermal range, +/− 2% of the detected temperature accuracy; 7.5 ÷ 13 μm spectral range; 1.36 mrad spatial resolution; 25◦ × 19◦ embraced field). The camera was also equipped with a 3.1 Mpixel photographic sensor that allowed the acquisition of the thermal image at the same time as the visible one, with the same shooting conditions. The images were acquired by positioning the IR camera frontally on the wall surface, a few meters away, in passive mode, thus framing the portion of the wall to be investigated and, at the same time, ensuring a good spatial resolution with a spot size of a few millimeters. The analyzed areas are shown in Fig. 2 and detailed in Table 1.

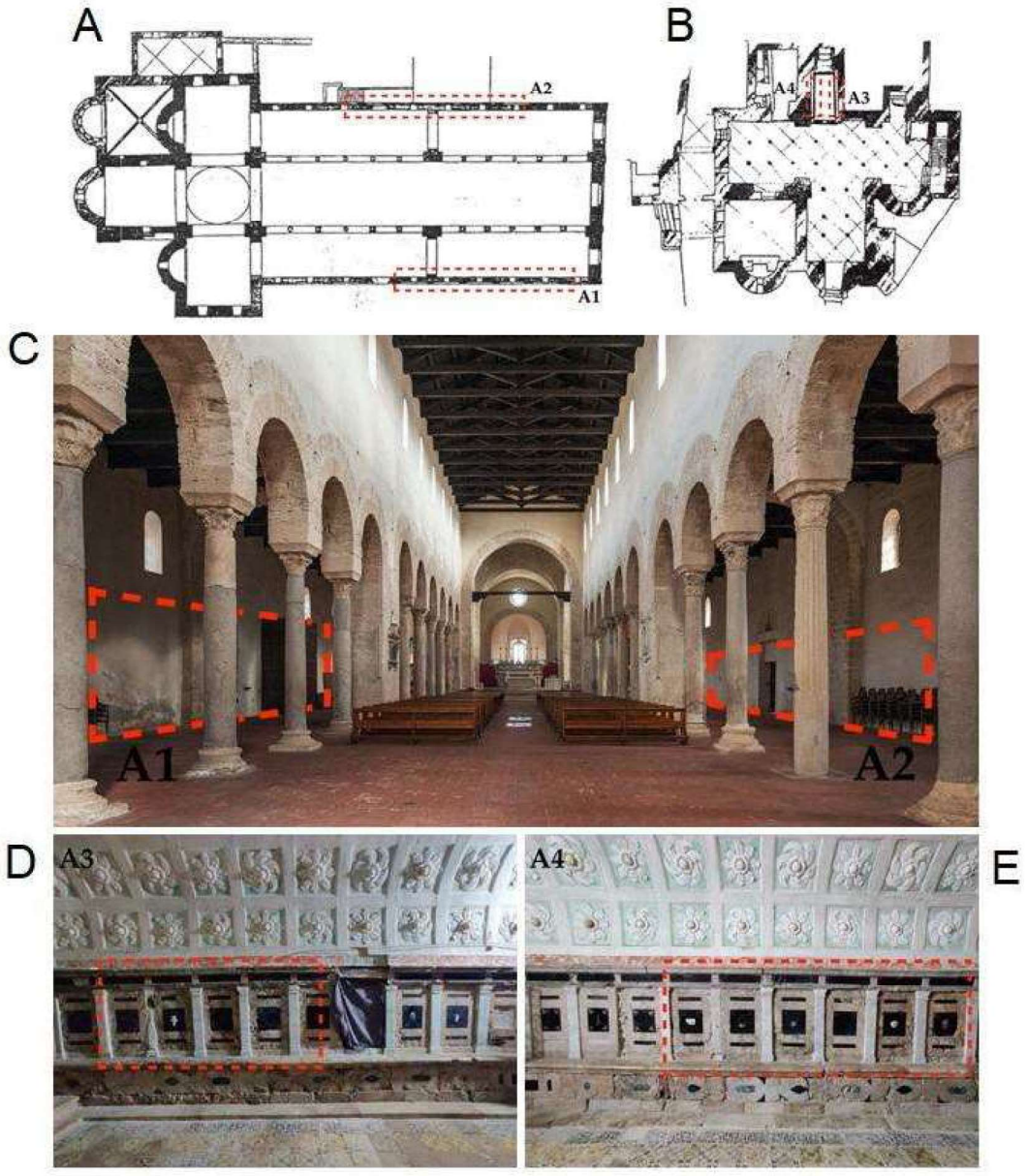

Figure 2. Plan of the two levels of the Gerace Cathedral: the three-aisled basilica (A), on the upper floor and the Crypt (B), located on the lower floor, with the areas of infrared thermography (IRT) measurements (A1-A4), and some representative images of the sampling areas (C-E). Upper level: (C) left (A1) and right (A2) aisles of the Cathedral; (D-E) the Madonna dell'Itria Chapel: left (A3) and right (A4) walls.

2.2 Micro-destructive laboratory methods and sampling

Minimal sampling was required for the laboratory-based surveys involving microscopic investigations by POM and SEM-EDS, as well as XRPD and IC. Then, a careful sampling of micro-fragments (sizes smaller than ~5 mm^2) and powders was carried out by selecting areas and collecting different types of representative samples (i.e., stones, plasters, pigments, and salt efflorescences). Minimally invasive procedures were followed for the latter, using suitable stainless-steel tools such as small tweezers, scalpels, and micro-scalpels. The sampling phase was performed on both levels of the building: the upper one, where the Cathedral is located, and lower one, which hosts the Crypt. All of the documentation with the sampling points, together with the type of material and the techniques used, are shown in Fig. 3 and in Table 1. The Polarized Optical Microscopy (POM) studies of thin stratigraphic sections were conducted in order to characterize the main materials present at the site, including the stones, mortars, and what remains of some ancient wall paintings. Observations were performed on twenty-four samples using a Primotech 40 (Primotech Zeiss) microscope coupled with a digital camera to capture images. The SEM-EDS analyses allowed us to investigate the samples in greater detail, both from a morphological and compositional point of view. Chemically (in terms of major elements), the method helped investigate not only the properties of the materials but also their associated alteration products [25]. Investigations were carried out on samples coated with a thin and highly conductive graphite film using an ultra-high-resolution SEM (ZEISS CrossBeam 350 equipment), coupled with an EDS – EDAX OCTANE Elite Plus - Silicon drift type detector. type. X-Ray Powder Diffraction (XRPD) is commonly used in materials science to determine the crystallographic structure of crystalline solids [26]. In this study, XRPD was specifically used to determine the mineralogical phases constituting the samples of salt efflorescences [27]. The analyses were performed with a Bruker D8 Advance X-Ray diffractometer (Bruker, Karlsruhe, Germany), with Bragg-Brentano geometry and a copper sealed tube X-ray source producing Cu kα radiation (wavelength of 1.5406 Å) from a generator operating at 40 kV and 40 mA. The diffracted X-rays were recorded on a scintillation counter detector located behind a set of long Soller slits/parallel foils. Scans were collected in the range of 3–65° 2θ, using a step size of 0.014° 2θ and a step counting time of 0.2 s. The EVA software (DIFFRACplus EVA version 11.0. rev. 0) was used to identify mineral phases by comparing experimental patterns with 2005 PDF2 reference patterns. Ion Chveronatography (IC) can be used to determine ion concentrations in an unknown sample [28]. In Cultural Heritage studies, as in this study, it has been used to identify the nature of the soluble salts and to quantify them [29]. A Dionex DX 120 equipment on a filtered supernatant (filter Minisart RC 25, diameter = 0.45 μm) provided the IC data, with the determination of the following ionic species: PO_4^{3-}, SO_4^{2-}, NO_3^-, Cl^-, F^-, Br^-, Li^+, NH_4^+, Na^+, K^+, Ca^{2+}, Sr^{2+} and Mg^{2+}. The determination of HCO_3^- was carried out by acid-base titration with HCl.

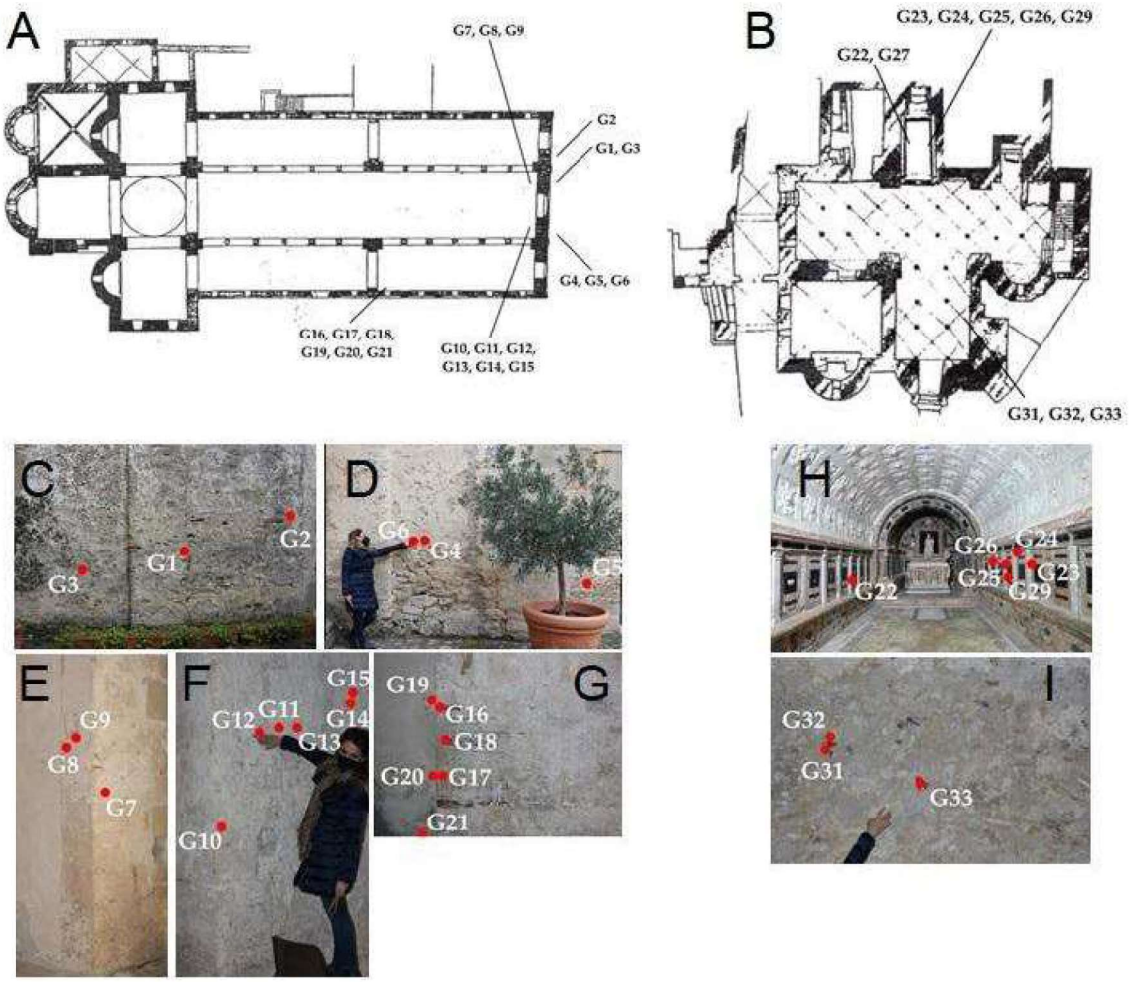

Figure 3. Plan of the two levels of the Gerace Cathedral: the three-aisled basilica (A), on the upper floor and the Crypt (B), located on the lower floor, with the location of the sampling points, and representative images of the sampling procedure (C-I). Upper level: (C-D) outside the Cathedral's main entrance (G1-G6); (E-F) inside, near the sides of the portal (G7-G15), and (G) on the internal wall of the left aisle (G16-G21). Lower level: (H) inside the Madonna dell'Itria Chapel (G22-G29) and (I) on the internal right wall of the apsidal entrance (G31-G33).

Table 1 Summary of areas investigated and sampled both with in-situ and laboratory-based methods. POM=Polarizing Optical Microscopy; IC=Ion Chromatography; XRPD=X-Ray Powder Diffraction; SEM-EDS=Scanning Electron Microscopy coupled with electron-dispersive spectroscopy; IRT=InfraRed Thermography

Area ID	Measurement area	Type	Employed Techniques
A1	Internal wall of cathedral, left aisle	Wall	IRT
A2	Internal wall of cathedral, right aisle	Wall	IRT
A3	Indoor/Madonna dell'Itria Chapel, right side	Wall	IRT
A4	Indoor/Madonna dell'Itria Chapel, left side	Wall	IRT
Sample ID	**Sampling area**	**Type**	**Employed Techniques**
G1	Outdoor/From the main entrance of the basilica	Mortar	POM; SEM-EDS
G2	Outdoor/From the main entrance of the basilica	Mortar	POM; SEM-EDS
G3	Outdoor/From the main entrance of the basilica	Mortar	POM; SEM-EDS
G4	Outdoor/From the main entrance of the basilica	Mortar	POM; SEM-EDS

G5	Outdoor/From the main entrance of the basilica	Stone material	POM
G6	Outdoor/From the main entrance of the basilica	Mortar	POM; SEM-EDS
G7	Indoor/From the portal of the basilica	Plaster	POM; SEM-EDS
G8	Indoor/From the portal of the basilica	Plaster + blackish pictorial film	POM; SEM-EDS
G9	Indoor/From the portal of the basilica	Plaster + blackish pictorial film	POM; SEM-EDS
G10	Indoor/From the portal of the basilica	Plaster + yellowish pictorial film	POM; SEM-EDS
G11	Indoor/From the portal of the basilica	Plaster + blackish pictorial film	POM; SEM-EDS
G12	Indoor/From the portal of the basilica	Plaster + brownish pictorial film	POM; SEM-EDS
G13	Indoor/From the portal of the basilica	Plaster + yellowish pictorial film	POM; SEM-EDS
G14	Indoor/From the portal of the basilica	Plaster + reddish pictorial film	POM; SEM-EDS
G15	Indoor/From the portal of the basilica	Plaster + beige-yellowish pictorial film	POM; SEM-EDS
G16	Indoor/From the left aisle of the basilica	Plaster + reddish pictorial film	POM; SEM-EDS
G17	Indoor/From the left aisle of the basilica	Plaster + green pictorial film	POM; SEM-EDS
G18	Indoor/From the left aisle of the basilica	Plaster + brownish pictorial film	POM; SEM-EDS
G19	Indoor/From the left aisle of the basilica	Salt efflorescences	IC; XRPD
G20	Indoor/From the left aisle of the basilica	Salt efflorescences	IC; XRPD
G21	Indoor/From the left aisle of the basilica	Salt efflorescences	IC; XRPD
G22	Indoor/Madonna dell'Itria Chapel, left wall	Salt efflorescences	IC; XRPD
G23	Indoor/Madonna dell'Itria Chapel, right wall	Salt efflorescences	IC; XRPD
G24	Indoor/Madonna dell'Itria Chapel, right wall	Salt efflorescences	IC; XRPD
G25	Indoor/Madonna dell'Itria Chapel, right wall	Salt efflorescences	IC; XRPD
G26	Indoor/Madonna dell'Itria Chapel, right wall	Stone material	POM
G27	Indoor/Madonna dell'Itria Chapel, right wall	Stone material	POM
G29	Indoor/Madonna dell'Itria Chapel, right wall	Stone material	POM
G31	Indoor/Right wall with respect to Crypt entrance	Plaster + reddish pictorial film	POM; SEM-EDS
G32	Indoor/Right wall with respect to Crypt entrance	Plaster + yellowish pictorial film	POM; SEM-EDS
G33	Indoor/Right wall with respect to Crypt entrance	Plaster + reddish pictorial film	POM; SEM-EDS

3. Results and Discussion

3.1 InfraRed Thermography

The IRT mapping of the surface thermal distribution supported the evaluation of the conservation state of the masonry [30,31], especially where damage forms were macroscopically considerable. The measurements carried out on the upper floor of the Cathedral, allowed a more accurate determination of the extent of the visible detachments between the layer of plaster and the underlying masonry. The thermographs revealed the presence of thermal discontinuities on both the left (frame A1 in Fig. 4) and right aisles (frame A2 in Fig. 4) of the Cathedral. These discontinuities are mainly located in the lower part of the masonry (up to a height of ~ 1.5 m), where manifestations

of damage (i.e., loss of surface material and white salt efflorescences) were also visible to the naked eye. The IRT images also highlighted superficial swellings and micro-cracks in the plaster, suggesting the presence of moisture in the walls and most likely the formation of sub-efflorescence. Rising damp is generally related to water infiltration and migration phenomena that seem to affect a significant part of the building. The crystallization of salts below the material surface (sub-efflorescence) will generally occur when the evaporation rate is greater than the migration rate of a solution towards the exterior of a material. The inverse process instead determines the formation of external efflorescence caused by the crystallization of deposited salts [32]. In more detail, the IR images of the investigated areas (frames A1 and A2 in Fig. 4) show that efflorescence phenomena can be detected by IRT; in fact, a correspondence can be observed between the areas with white salt efflorescence and surface temperature anomalies with respect to the surrounding masonry portions. Cooler temperatures (from cyan to dark blue on the colors scale i.e., less heat and infrared radiation emitted) are found in the lower part of the masonry (up to ~30 cm in height), as shown by the vertical temperature profiles in the figure, which is certainly more exposed to environmental cooling as well as being subject to capillary rising phenomena and efflorescence. Otherwise, warmer sectors (from orange to red on the color scale, i.e., emitting more heat and infrared radiation) are found where the masonry shows a lower degree of weathering, namely in those portions of the wall that are not affected by efflorescence but by micro-cracking, flaking, and detaching phenomena (at a height between 30 cm and 1.50 m). Thermographs of the Crypt, whose walls are covered with slabs of stone materials of various kinds, allowed us to carry out the first mapping of the presence of moisture in the masonry and to relate it to the possible presence of dissolved salts that could cause alteration phenomena. In many cases, the ornamental slabs showed an evident detachment from the wall, probably as a result of mechanical stress due to the presence of moisture and the consequent formation of salts especially as sub-efflorescences. For example, the thermal image related to the right wall of the Crypt (frame A3 in Fig. 4) shows evident cracks near the hotter areas (reddish-yellow tones on the color scale and a temperature around 0.25 °C greater than in the cooler areas) indicating an advanced degradation of the covering materials up to detachments in small parts.

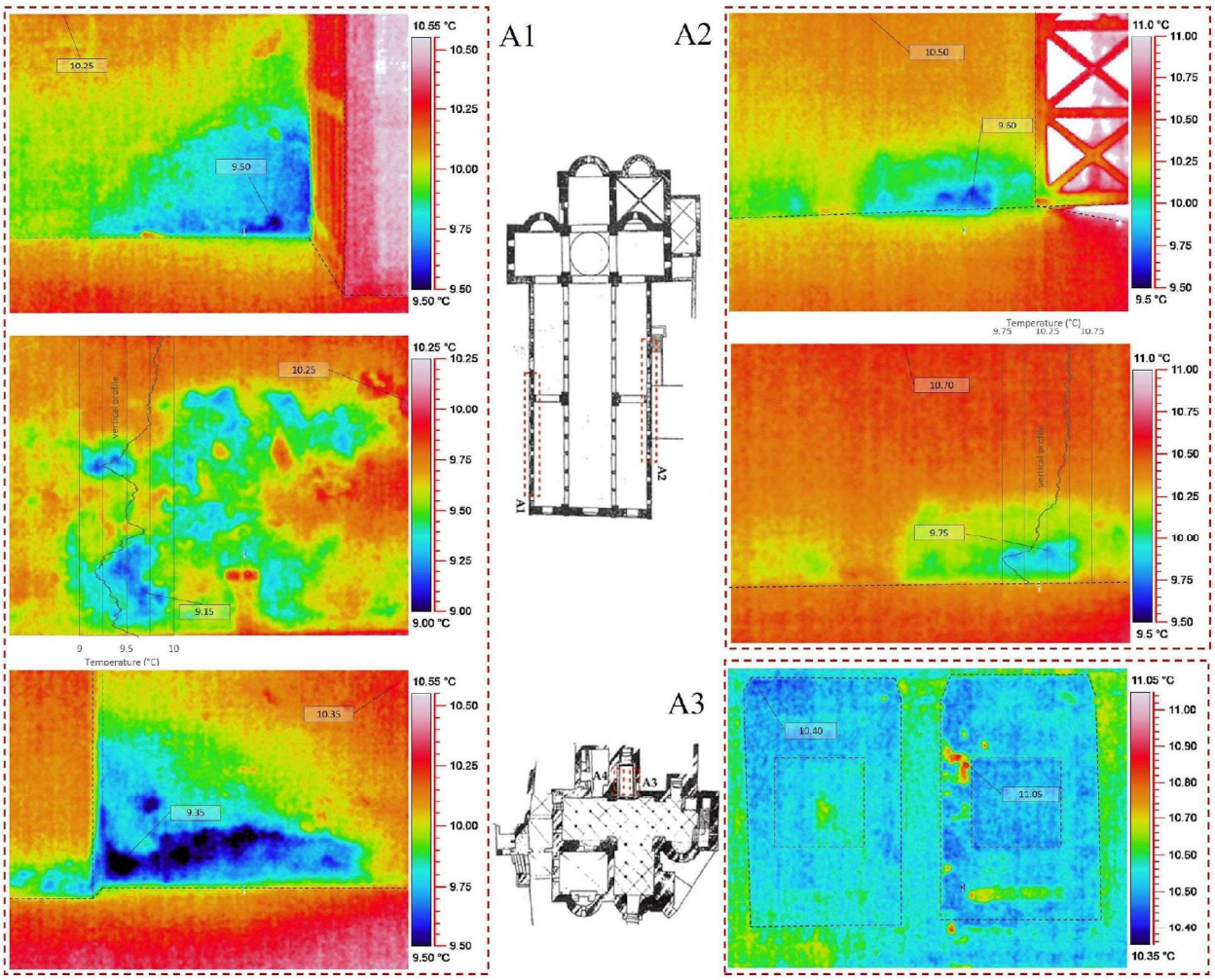

Figure 4. Representative infrared thermography (IRT) images of the investigated areas. Upper level: left (Zone A1) and right (Zone A2) aisles of the Cathedral. Lower level: right wall inside the Madonna dell'Itria Chapel (A3). The highest and lowest temperatures are reported in the boxes for all IRT images. The vertical temperature profiles are sketched both for the right and left aisles (gray lines). In addition, the edges of the walls and other decorative elements are delineated with thin black dashed lines for a better understanding. Note: Visible images of investigated areas by IRT are shown in Figure 2

3.2 Micro-Destructive Laboratory Methods

Thin section of 24 micro-fragments were manufactured for petrographic analysis. Observation under POM allowed us to identify the main minero-petrographic and textural features of the stones, mortars, and plasters with pictorial films, as well as evaluating their state of conservation. The petrographic results are described for each of the samples, highlighting their main features, which serve to link or separate them from each other; in fact, where they are similar, the samples are described as a single group. Some representative photomicrographs are shown in Figure 5, while Table S1 reports the main petrographic features detected for each sample.

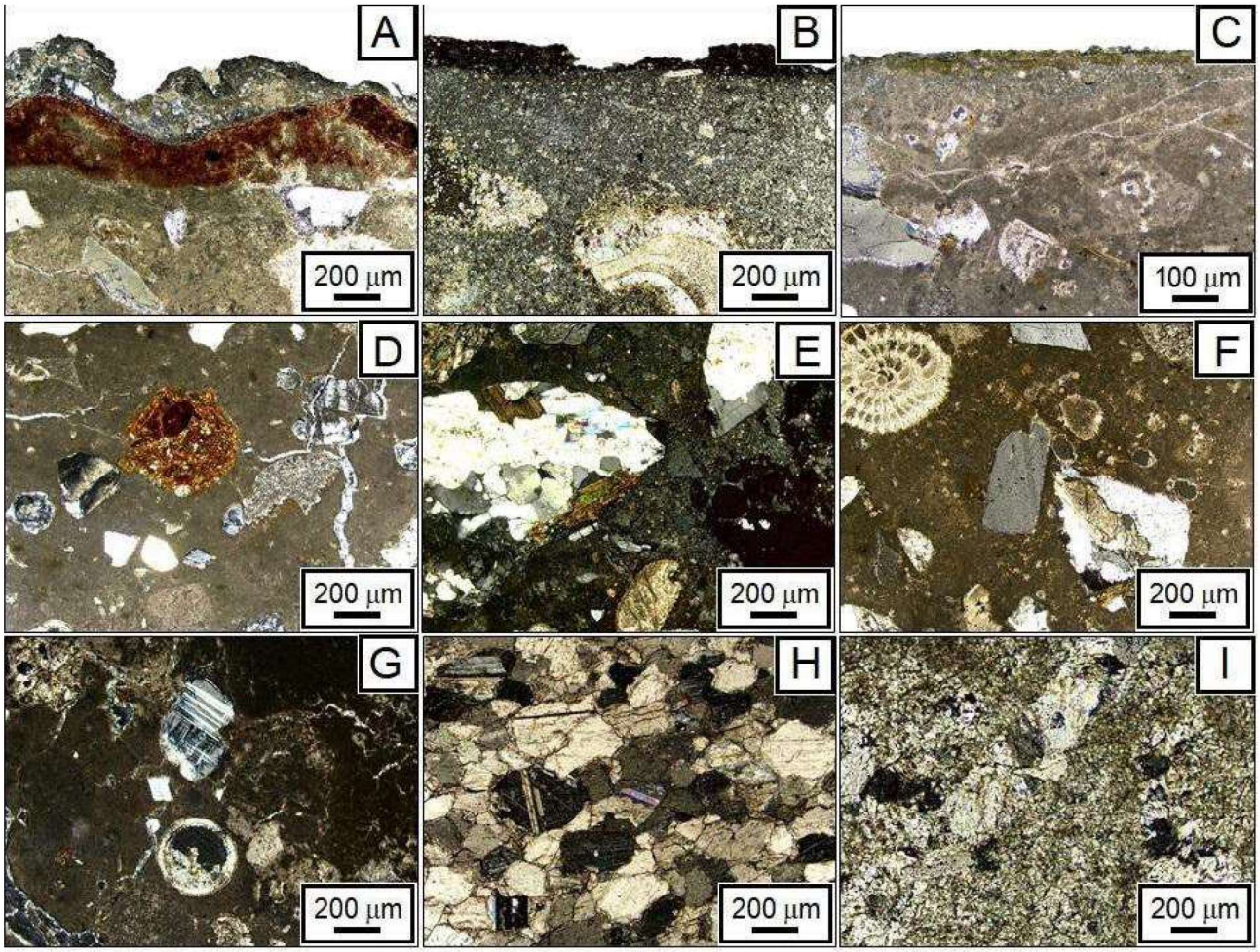

Figure 5. Representative cross-polarized light (CPL) photomicrographs of the studied samples; G31 (A) – Group 3/Type P/PF: sample stratigraphy with evidence of the three layers, i.e., plaster, reddish pictorial film and the *scialbo*; G12 (B) - Group 3/Type P/PF: sample stratigraphy with evidence of two layers, i.e., plaster and the brownish pictorial film; G32 (C, F) - Group 3/Type P/PF: sample stratigraphy with evidence of two layers, i.e., plaster and the yellowish pictorial film; G4 (D) - Group 2/Type M: detail of the mortar samples with quartz crystals, cocciopesto, and rock fragments; G7 (E) - Group 3/Type P/PF: detail of the plaster layers with quartz crystals and granitoid rock fragments; G6 (G) - Group 2/Type M: detail of the mortar samples with quartz crystals, granitoid rock fragments, and bioclasts; G29 (H) - Group 1/Type S: fine grained "mosaic" type marble; G27 (I) - Group 1/Type S: microcrystalline limestones calcite veins.

3.2.1 Group 1 - Samples G5, G26, G27, & G28: Stone Materials (Type S)

This group includes different kinds of stone materials (i.e., rock) present in the historic building, taken both from the Crypt and from the upper basilica (Figures 5H, GI; Table S1). Specifically, sample G5, which was obtained from an external area near the portal of the basilica, represents the constituent material with which the Cathedral is built. It is a bioclastic calcarenite containing abundant bioclasts as well as single crystalline inclusions, and rock fragments. Specifically, quartz crystals, micas (both biotite and muscovite), and oxides were identified together with fragments of metamorphic rocks, carbonate lithoclasts, and rare granitoids. All grains are bound together by a fine-grained calcite (micrite). The porosity is both primary and secondary (15%), with evident fillings by secondary recrystallized calcite. Accordingly, the stone sample can be classified as a biocalcarenite or packstone [33, 34]. The data are also consistent with the literature [35, 36], according to which this kind of stone is widely used in the Gerace area as a constituent material of the large-scale built cultural heritage. Samples G26 and G27, obtained from the ornamental slabs that cover part of the Crypt's walls, are microcrystalline limestones which host calcite veins made up of well-

formed crystals. The samples are in an advanced state of alteration with evident microfractures and secondary porosity. Finally, sample G29, s from a covering slab of the Crypt, is a marble characterized by a fine grain size (MGS <1mm;) and a generally homeoblastic (Ho) texture. The fabric is commonly of "mosaic" type, with small to very small crystals, which in some places form triple point junctions (120°). Slightly lineated or weakly oriented fabrics were also observed. The grain size ranges from 0.1 mm to 0.9 mm, often with clear traces of cleavage, while the grain boundary shape (GBS) varies from curved to straight. A shape preferred orientation (SPO) of the grains was not observed nor were accessory minerals.

3.2.2 Group 2 - Samples G1, G2, G3, G4, & G6: Mortars (Type M)

All the samples belonging to Group 2, were taken from the external facade of the building, at the entrance to the upper basilica (Figures 5D, 5G; Table S1). They are mortars characterized by a brownish micritic binder in Crossed Polarized Light (CPL), in which the aggregate fraction varies from well-sorted to moderately and poorly selected, and mainly consists of mono- and polycrystalline quartz crystals, micas, calcite, and various bioclasts. Like other inclusions, feldspars, oxides, and rare pyroxenes are present to a lesser extent. Fragments of volcanic (granitoids), metamorphic, and carbonate rocks were also detected. All samples, except for G4 and G6, contain a layer of finishing mortar (layer B) with the same mineralogical composition as the main layer (layer A) but with a finer grain size. Samples G1, G2, and G4 also host sporadic cocciopesto inclusions. In terms of size, individual mineralogical phases vary from 400 μm to 1500 μm, while rock fragments reach dimensions of up to 2800 μm, with angular to sub-angular and to rounded to sub-rounded shapes. Fractured lumps with defined edges were also detected in all the samples, having a sub-spherical shape with diameters ranging from 400μm to 2000μm. The presence of a finishing layer in samples G1, G2, and G3 could be related to a previous restoration procedure which was probably carried out to consolidate the limestone ashlars. Unfortunately, there is no documentation of past restoration interventions in the archives, but oral sources suggest various interventions to the building over time.

3.2.3 Group 3 - Samples G7, G8, G9, G10, G11, G12, G13, G14, G15, G16, G17, G18, G31, G32, & G33

Plasters with pictorial films (Type P/PF). The samples belonging to this group consist of plasters (layer A), covered with a very thin layer of pictorial film (layer B – up to 260 μm) (Figures 5A, 5B, 5C, GF; Table S1). Some specimens contain a finishing layer, probably a "*scialbatura*" (layer C - up to 350 μm) (samples G8, G10, G11, G14 and G31). More specifically, the term "*scialbatura*" or "*scialbo*" refers to a layer of light, fine, and thin plaster covering a mural painting. From a mineralogical point of view, layer A consists of a plaster containing a fairly homogeneous micritic binder (sometimes cryptocrystalline) in which the aggregate fraction varies from well-sorted to moderately and poorly selected. The coarse fraction is mostly constituted by monocrystalline quartz granules and polycrystalline ones, followed by micas, calcite, bioclasts, iron oxides, and rare feldspars, with sizes reaching 1400μm and shapes varying from angular to sub-angular and to rounded to sub-rounded. Fragments of rocks (volcanic, metamorphic, and calcareous) and rare cocciopesto with sizes reaching 4050 μm were also detected. The percentage of the aggregates in layer A varies from 20 % to around 50 % (by area) [37]. The latter was assessed by means of a semi-quantitative visual estimation. The porosity of the same layer A varies from about 5 to 15% (by area) and it consists of both primary and secondary pores with sizes of up to 700μm. In addition, recrystallization phenomena of the calcite were observed in the voids. The pictorial layer (layer B) appears to be very thin, sometimes with sporadic crystals of calcite occurring together with oxides. The color of the different samples appears

to be reddish to brownish and yellowish under Plane Polarized Light (PPL). Finally, layer C, where present consists of microcrystalline calcite, with thicknesses of up to 350 μm.

The SEM-EDS analyses were performed on thin and stratigraphic sections of the samples belonging to Group 2 (Type M) and Group 3 (Type P/PF) (Figure 5, Table S1). The binder's composition in the different layers, the raw materials, and the stratigraphy were investigated, paying special attention to the pigmented layers and the overlying ones (*scialbo*), where present.
For the Group 2 samples (G1-G4, G6) and those consisting of mortars, the morphological observations by SEM confirmed the OM data, highlighting the presence of two overlapping mortar layers for all the samples, except for G4 and G6. Five EDS measurements were performed on the binders of each layer present in the samples, and the average values were considered as representative of their chemical compositions (since no significant variations were observed when calculating the standard deviation relative to the mean values of the EDS dataset). Regarding the major elements, a large amount of CaO was detected in all the samples, in addition to significant SiO_2 and MgO concentrations, followed by lower amount of Al_2O_3 and Na_2O. The presence of Mg suggests that the lime was likely formed through the calcination of magnesian limestone and/or dolostone. This latter assumption was further confirmed by the EDS measurements performed on lumps (three spot analyses in their central portion to reduce contamination), suggesting the use of magnesian lime-based mortars. Furthermore, considerable amounts of Sr and SO_4 were also present, which may have been related to the use of evaporites as raw materials. In fact, celestine minerals (sulfates) were also found sporadically in the aggregate fraction and these may have precipitated as euhedral crystals after the liberation of Sr [38-40]. This could also indicate that the original raw materials were sourced from Gerace area [35, 36].
The morphological investigations of the samples belonging to Group 3 further with the OM data. Furthermore, the study of the binders conducted on the layers of plaster (layers A) revealed a chemical composition similar to that of the mortars of Group 2, confirming the use of the same raw materials for the plastering production. Specifically, our results suggested the presence of a magnesian lime-based plaster in all the samples, resulting from the calcination of Mg-limestones. In layer B, elements such as Si, Al, Mg, and K were mainly detected in blackish, brownish, green, and beige-yellowish pictorial films (samples G8, G9, G10, G11, G12, G13, G15, G17, G18). In addition, Fe was also detected in the beige-yellowish pictorial layers (G10, G13, G15, G32). Such elements are compatible to the possible use of raw materials from clay and other minerals that are commonly found in soils and were likely used as pigmenting compounds [41-47]. The EDS analyses of the reddish layers (samples G14, G16, G31, G33) highlighted mainly the presence of Hg and S (Figure 6-G31_c) along with elements attributable to earthy pigments, suggesting the use of a mixture of cinnabar or vermillion [30] with oxide and/or clay-based pigments; in fact, morphologically, the reddish pigmenting agents are heterogeneously distributed within the layers (Figure 6; G31_b). Finally, the C layers (*scialbo*), where present, always consisted of $SrSO_4$ and CaO for all analyzed samples (Figure 6; G8_b and G8_c).

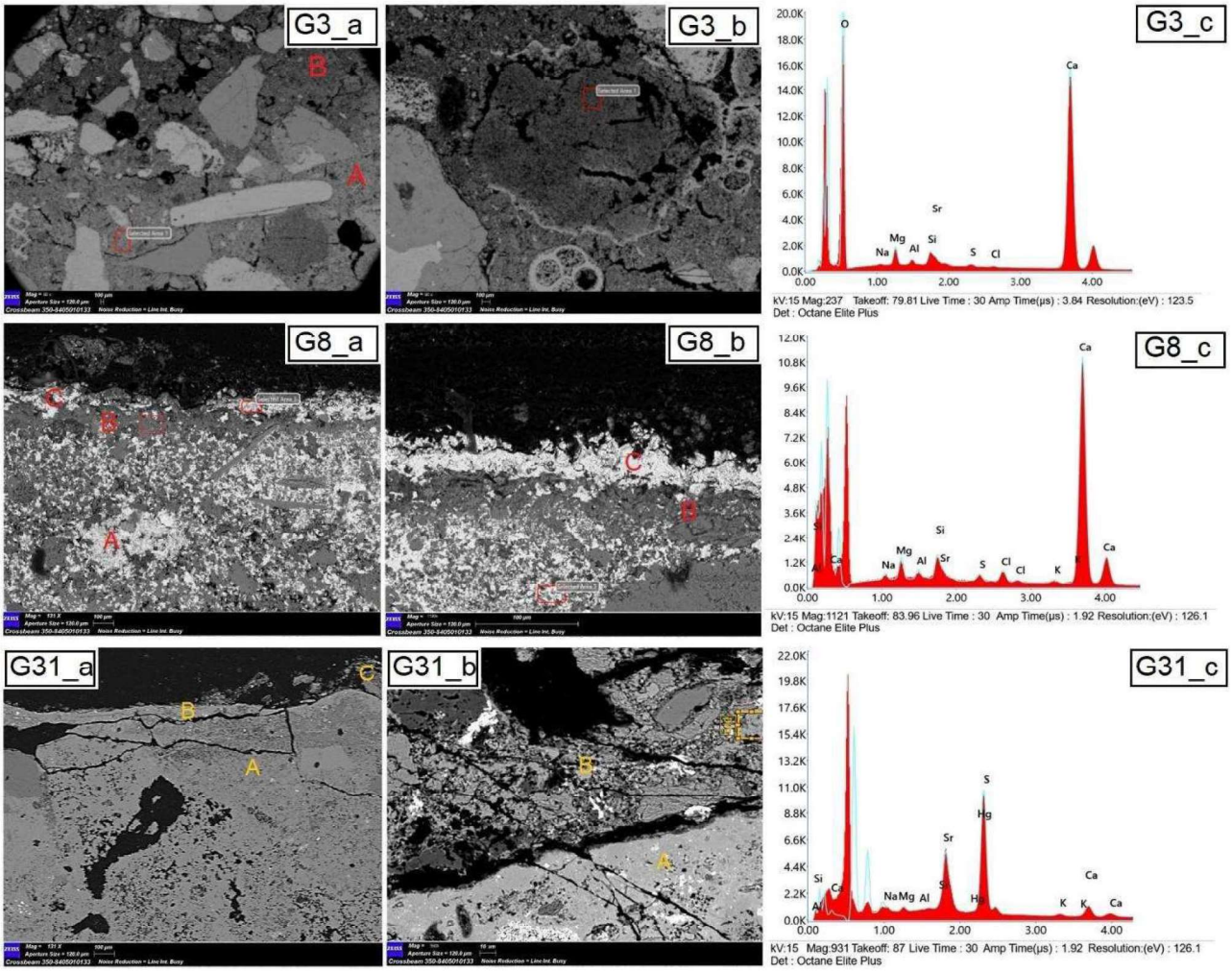

Figure 6. Representative scanning electron microscopy (SEM) images of thin sections showing the stratigraphy and details of the studied samples; G3_a) sample G3 with evidence of two layers named (A) and (B); G3_b) sample G3 with evidence a fractured lump with defined edges; G3_c) electron-dispersive spectroscopy (EDS) spectrum of sample G3 detected in the binder of layer A; G8_a) sample G8 with evidence of three layers named (A-plaster), (B-pictorial film), and (C-*scialbo*); G8_b) sample G8 with clear evidence of the two most superficial layers (B and C); G8_c) EDS spectrum of sample G8 detected in layer C (*scialbo*) where the brightest features represent celestine crystals (SrSO4); G31_a) sample G31 with evidence of three layers named (A-plaster), (B-pictorial film), and (C-*scialbo*); G31_b) sample G31 with clear evidence of layers named (A) and (B); G31_c) EDS spectrum of sample G31 detected in the pigmented layer B (reddish layers) showing a poor distribution of pigmenting agents.

The IC analyses allowed us to investigate the ionic species contributing to the damage within the walls. In general, the damage caused by soluble salts in building materials can be produced as a result of several mechanisms based on the kind of crystallization taking place [48]. The soluble fraction of major anions for all the analyzed samples mainly consisted of sulfate (SO_4^{2-}) and hydrogen carbonate (HCO_3^-), as well as lesser amounts of nitrate ions (NO_3^-) and chloride (Cl^-); among the cations, Na^+ and Ca^{2+} were the most abound in all samples, followed by less abundant K^+ and Mg^{2+}, along with traces of Sr^{2+}.

A preliminary analysis of the data (Figure 7) suggested that sulfates and carbonates were the main soluble species present in the investigated areas followed by nitrates and chlorides. For the sulfates, the overall data suggested the presence of sodium sulfates, as well as lower amounts of calcium and magnesium sulfates. Significant differences between the soluble species detected in the samples of the main Cathedral (G19-21) and those of the Crypt (G22-25) should be underlined. Specifically, the samples from the Crypt contained low concentrations of alkaline ions (i.e., Na^+, K^+), possibly due to

the greater humidity that generally prevails in an underground environment; such conditions can inhibit the precipitation of sodium/potassium salts, since the latter are generally more soluble than calcium/magnesium salts [49]. Considering the scarcity evidence of sodium ions and the low magnesium ion contents, gypsum may have crystallized as one of the main salts in the Crypt samples, but not the only one. Indeed, gypsum may form if the relative humidity of an environment becomes lower than the relative humidity at equilibrium (RHeq) of the saturated salt solution in the system [50]. In fact, among the recognized salts, the gypsum has the highest deliquescence RH, which is around 99.6% at 20°C [51], implying that such a phase is stable even under extremely humid conditions [41].

However, the calcium sulfate (gypsum) could have different origins; for example, it can derive from the original materials (i.e., building materials, rocks, raw materials) or have a different source altogether (i.e., environment). Both options were feasible in this study. The gypsum may have originated from the plaster covering the wall surfaces or from the soil surrounding the building; in the latter case, the sulfate species may have been dissolved in soil water and may have crystallized on the wall surfaces through capillary action.

For the carbonates, Ca was the second most abundant cation in the samples, which could be partly attributed to the intrinsic composition of the investigated materials and/or to their long-term coexistence with lime-rich materials (e.g., plasters, lime mortars) under moist conditions.

In addition, the presence of magnesium sulfate could not be excluded for the Crypt samples G22 and G23. For the latter two, values between 34 and 48 ppm were detected against a threshold of less than 9 ppm detected for all other samples.

When evaluating the contribution of the other soluble species detected by IC, the presence of nitrates in all the samples analyzed, albeit in minimal concentrations, should also be noted. Nitrates, such as potassium and calcium nitrate, can originate from soils through microbiological activity decomposing organic nitrogenous products. The presence of nitrates in masonry, as well as for the other salts, is in accordance with the rising damp phenomena described by Arnold and Zehnder [49] in a scheme showing the vertical fractionation of soluble salt species on a wall; the most soluble and hygroscopic salts (e.g., magnesium and calcium nitrates) reached higher heights on the surface of the wall than less soluble and less hygroscopic salts (e.g., sulfates) which accumulated in the lower portions of the masonry. Even chlorides, like nitrates, are highly soluble and may cause serious damage in the presence of high moisture contents within masonry due to their hygroscopicity. This may lead to decay phenomena that generally occur in masonry with high and permanent moisture contents. The IC results are summarized in Figure 7.

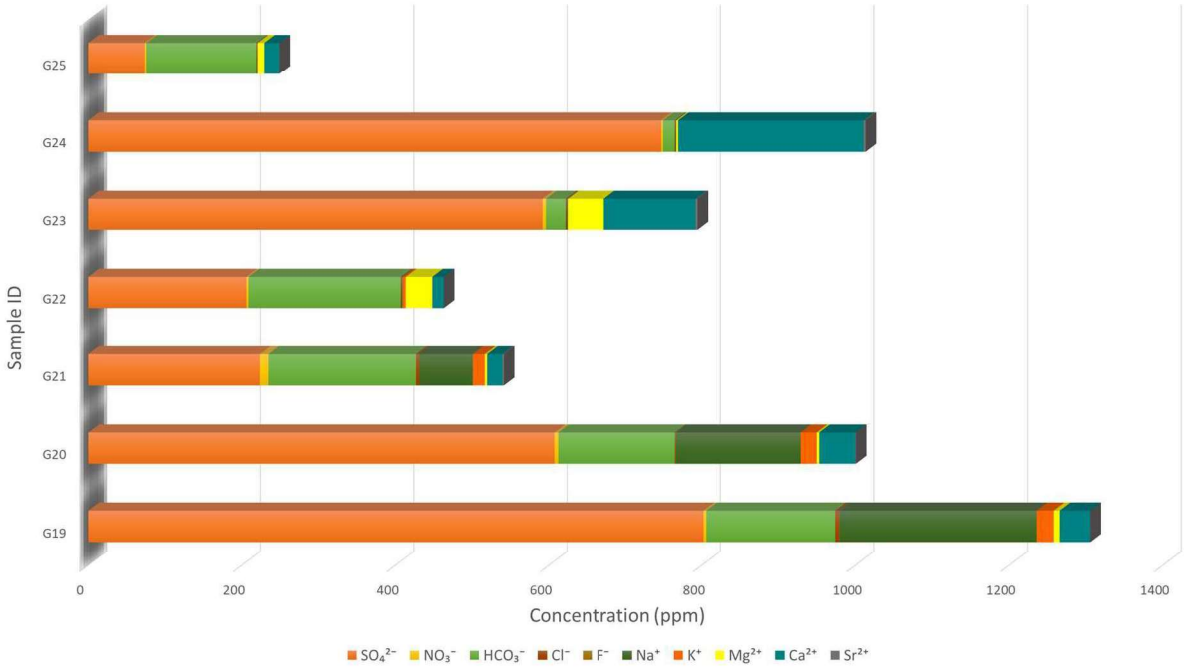

Figure 7. Concentrations of ionic species expressed in ppm

The XRPD analysis of the efflorescence samples (G19-G25) revealed that calcite was the dominant phase in all the samples from the Crypt, except for G23 and G24. Among other more abundant crystalline phases, the following were detected: thenardite (sodium sulfate) only in the Cathedral samples (G19-G21); gypsum (calcium sulfate) in all samples except in G19 (from the Cathedral) and hexahydrite (magnesium sulfate hexahydrate) in all samples of the Crypt except in G24. Non-soluble minerals such as quartz, clay minerals, magnesite, hydromagnesite, and feldspars were also identified in low concentrations. The data support the IC investigation suggesting that sulfates and carbonates are the most abundant soluble phases.

As for the sulfates, thenardite was exclusively present in the samples of the main Cathedral while hexahydrite and gypsum occurred in those from the Crypt. Traces of gypsum were also found in the Cathedral samples, namely G20 and G21. The origin of these salts could be linked to the interaction (weathering) between capillary rise water and the stone/plaster substrates. Elements such as Mg^{++}, Na^{+}, SO_4^{2-} and Ca^{++} are preferentially leached from substrates, recombining under specific microclimatic conditions in the efflorescences salts following their mobilization through the pore network of the substrates. The presence of calcite has resulted from the carbonate substrate or to the lime-based plaster covering the building's surface, while the quartz, clay minerals, and feldspars could have been related to the composition of the mortar/plaster (sandy aggregates). Sulfate salts act as rock-decaying agents which may lead to a poor state of cultural heritage conservation. As is well known, one of the major causes of rock decay in nature [52] and weathering of natural and/or artificial building material [53-55] is the presence and crystallization of these soluble salts from repeated cycles of crystallization/dissolution within the matrix of porous stone materials. Furthermore, differences in the semi-quantitative estimates of the mineral phases recognized in the two sampled areas may depend on various factors such as differences in sampling heights on the masonry, the interaction of the samples with adjacent materials of diverse nature, environmental conditions, as well as different levels of mobility and the migration of salts through the masonry [49]. The results of the XRPD analyses are summarized in Table 2.

Table 2. Minerals occurring in the analyzed samples. Notes: Thn=Thenardite; Cal = Calcite; Qtz = Quartz; Hhy = Hexahydrite; CM = Clay Minerals; Gy = Gypsum; Hmgs = Hydromagnesite; Mgs = Magnesite; Fs = Feldspars; xxx = abundant; xx = moderate; x = poor; r = rare.

Samples	Thn	Cal	Qtz	Hhy	CM	Gy	Hmgs	Mgs	Fs
G19	xxx	xx	x	-	r	-	-	-	-
G20	xxx	xx/x	r	-	r	x	r	r	-
G21	xxx/xx	xxx	r	-	r	r	-	-	r
G22	-	xxx	-	xx/x	x	-	-	-	-
G23	-	-	-	xxx/xx	-	xxx	-	-	-
G24	-	-	-	-	-	xxx	-	-	-
G25	-	xxx	-	r	-	x	-	-	-

4. Conclusions

A multidisciplinary approach employing non-destructive and micro-destructive methods was adopted to assess the state of conservation of the Gerace Cathedral. The results showed that:

- The IRT method is a useful non-contact tool that could be applied for a rapid preliminary evaluation of the weathering state of the building. The technique allowed a preliminary zonation and mapping of the weathering processes affecting the Cathedral's masonry. Such non-destructive methodologies are particularly relevant when studies must be conducted rapidly, especially for preliminary assessments or monitoring purposes when imminent restoration work is expected. It is worth underlining that the reported data herein refer to preliminary surveys and further studies should be performed to investigate the thermo-hygrometric conditions of the historical building.

- The IC and PXRD analyses of salt efflorescence samples helped confirm that salts contribute to the deterioration of the stones, walls, and mural paintings of the Cathedral, resulting in weathering products of cultural heritage materials. Specifically, salt accumulations in walls mainly originated from the ions leached from rocks, soils, stone, and other raw materials used in the building. Overall, the application of the IC analytical procedure allowed us to quantify the amounts of major cations and anions. The analytical data suggested that sulfates and carbonates are the most abundant soluble species present in the two investigated areas, followed by nitrates and chlorides. Furthermore, the concentrations of the different species were notably different between the two sampled environments, i.e., the Crypt and the upper basilica. These differences were closely related to the environmental conditions, such as the higher humidity of the underground environment. The mineralogical studies by XRPD were in full agreement with the IC results.

- Microscopic observations by OM allowed us to distinguish different layers among samples and especially those with a pictorial film. In general, in all samples contained similar raw materials, especially those belonging to Groups 2 and 3, confirming a local origin. The presence of a finishing layer of mortar found only in some samples from Group 2 also suggested that an undocumented restoration intervention probably took place in the past. The rock samples (Group 1), on the other hand, were characterized as marbles and crystalline limestones. In the latter case, it was impossible to establish their provenance and further studies will thus be conducted on these materials of unknown origin.

- The SEM-EDS investigations revealed the presence of similar elements/compounds for all the examined samples, attesting to the use of Mg-lime-based plasters/mortars and lime derived from the calcination of carbonates of evaporitic origin. The layers of *scialbo* exhibited the same composition, and this material probably derived from previous undocumented restoration interventions. In the painted layers, on the other hand, inorganic chromophores based on natural mineral pigments were found to produce blackish, brownish, green, and yellow shades of color. The use of cinnabar or vermilion, mixed with earthy pigments, was confirmed for the reddish layers.

Finally, this work allowed us to characterize and preliminarily evaluate the state of conservation of the Gerace Cathedral building materials, providing useful data for the planning of future restoration interventions. In fact, in the context of scientific research conducted on Cultural Heritage, the approach represents a necessary prerequisite for planning the best restoration and protection plan possible. A holistic and integrated approach should always be followed for the preservation of cultural heritage, prior to any restoration interventions. Further studies will be conducted to acquire a better understanding of other pilot areas within the Cathedral suffering from a poor state of conservation.

References

1. E.T. Delegou, G. Mourgi, E. Tsilimantou, C. Ioannidis, A. Moropoulou, A Multidisciplinary Approach for Historic Buildings Diagnosis: The Case Study of the Kaisariani Monastery. Heritage 2019, 2, 1211-1232. https://doi.org/10.3390/heritage2020079.
2. A. Moropoulou, K.C. Labropoulos, E.T. Delegou, M. Karoglou, A. Bakolas, Non-destructive techniques as a tool for the protection of built cultural heritage, Construction and Building Materials, Volume 48, 2013, Pages 1222-1239 https://doi.org/10.1016/j.conbuildmat.2013.03.044.
3. F. Sandrolini, E. Franzoni, G. Cuppini, L. Caggiati, Materials decay and environmental attack in the Pio Palace at Carpi: A holistic approach for historical architectural surfaces conservation, Building and Environment, Volume 42, Issue 5, 2007, Pages 1966-1974, https://doi.org/10.1016/j.buildenv.2006.04.021.
4. F. Sandrolini, E. Franzoni, E. Sassoni, P.P. Diotallevi. The contribution of urban-scale environmental monitoring to materials diagnostics: A study on the Cathedral of Modena (Italy), Journal of Cultural Heritage, Volume 12, Issue 4, 2011, Pages 441-450, https://doi.org/10.1016/j.culher.2011.04.005.
5. L. Berto, A. Doria, P. Faccio, A. Saetta, D. Talledo. Vulnerability Analysis of Built Cultural Heritage: A Multidisciplinary Approach for Studying the Palladio's Tempietto Barbaro, International Journal of Architectural Heritage, 2017, 11:6, 773-790, DOI: 10.1080/15583058.2017.1290853.
6. E. Spoldi, I. Ippolito, A. Stella, S. Russo. Non-destructive techniques for structural characterization of cultural heritage: A pilot case study. Struct Control Health Monit, 2021, 28, 12. https://doi.org/10.1002/stc.2820.
7. V. Cataldo, Gerace. La Cattedrale, Nosside, 2001.
8. G. Occhiato, Le Chiese dell'età normanna alle forme rinascimentali, in: I Beni culturali e le chiese di Calabria, Laruffa, Reggio Calabria, 1981, pp. 346.
9. C. Bozzoni, L'organismo architettonico, in: S. Gemelli, C. Bozzoni, La Cattedrale di Gerace, Cassa di risparmio di Calabria e Lucania, Effesette, Cosenza, 1986, pp. 84-99.
10. E. Guidoboni, G. Ferrari, G. Tarabusi, G. Sgattoni, A. Comastri, D. Mariotti, C. Ciuccarelli, M.G. Bianchi, G. Valensise, (2019), CFTI5Med, the new release of the catalogue of strong earthquakes in Italy and in the Mediterranean area. Sci Data 6, 80, 2019. https://doi.org/10.1038/s41597-019-0091-9. doi: https://doi.org/10.1038/s41597-019-0091-9
11. A. Costanzo, A. D'Onofrio, F. Silvestri, Seismic response of a geological, historical and architectural site: the Gerace cliff (southern Italy). Bull Eng Geol Environ 78, 5617–5633, 2019. https://doi.org/10.1007/s10064-019-01515-0
12. C. Bozzoni, Calabria Normanna, Ricerche sull'architettura dei secoli undicesimo e dodicesimo, Officina, Roma, 1974.

13. P. Pensabene, Marmi di rimpiego, in: La Cattedrale di Gerace, Cassa di risparmio di Calabria e Lucania, Effesette, Cosenza, 1986, pp. 127-143.
14. F. Mosino, Storia linguistica della Calabria, I, Marra, Cosenza, 1988, p. 91.
15. G. Occhiato, Il Soccorpo in: La Cattedrale di Gerace, Cassa di risparmio di Calabria e Lucania, Effesette, Cosenza, 1986, pp. 84-99.
16. G. Occhiato, Interpretazione della cripta del duomo normanno di Gerace in Calabria, in: Byzantion, Tomo XLIX, 1979, pp. 314-362.
17. P. Orsi, Le chiese basiliane della Calabria, Firenze, Vallecchi, 1929.
18. C. Genovese, I grandi monumenti per la valorizzazione dei beni culturali in Calabria. Il caso della Cattedrale di Gerace, in: Reuso: La cultura del restauro e della valorizzazione. Temi e problemi per un percorso internazionale di conoscenza, 2° Convegno Internazionale sulla documentazione, conservazione e recupero del patrimonio architettonico e sulla tutela paesaggistica, Alinea Editrice, Firenze, 2014.
19. F. Mercuri, C. Cicero, N. Orazi, S. Paoloni, M. Marinelli, U. Zammit, Infrared Thermography Applied to the Study of Cultural Heritage. Int. J. Thermophys 2015, 36, 1189–1194. https://doi.org/10.1007/s10765-014-1645-x
20. A. Moropoulou, N.P. Avdelidis, M. Karoglou, E.T. Delegou, E. Alexakis, V. Keramidas, Multispectral Applications of Infrared Thermography in the Diagnosis and Protection of Built Cultural Heritage. Appl. Sci 2018, 8, 284. https://doi.org/10.3390/app8020284
21. C. Meola, G.M. Carlomagno, Recent advances in the use of infrared thermography. Meas. Sci. Technol. 2004, 15, R27.
22. C. Ibarra-Castanedo, J.R. Tarpani, X.P. Maldague, Nondestructive testing with thermography. Eur. J. Phys. 2013, 34, S91.
23. A. Costanzo, M. Minasi, G. Casula, M. Musacchio, M.F. Buongiorno, Combined Use of Terrestrial Laser Scanning and IR Thermography Applied to a Historical Building. Sensors, 2015, 15, 194-213. https://doi.org/10.3390/s150100194
24. C. Balaras, A. Argiriou, Infrared thermography for building diagnostics. Energy Build. 2002, 34, 171–183.
25. C. Walker, I. Joosten, Introduction: Analysis of Cultural Heritage, in: Microscopy and Microanalysis, 2011, 17 (5), 655-655. doi:10.1017/S1431927611012062
26. C. Cardell, D. Benavente, J. Rodríguez-Gordillo, Weathering of limestone building material by mixed sulfate solutions. Characterization of stone microstructure, reaction products and decay forms. Materials Characterization, 2008, 59, 1371-1385
27. A. Ali, Y.W. Chiang, R.M. Santos, X-ray Diffraction Techniques for Mineral Characterization: A Review for Engineers of the Fundamentals, Applications, and Research Directions. Minerals, 2022, 12, 205. https://doi.org/10.3390/min12020205
28. J. Weiss, Handbook of Ion Chromatography. 4th ed.; Wiley-VCH, 2016. ISBN: 978-3-527-32928-1
29. A. Alvarez de Buergo, M.P. Lopez-Arce, R. Fort, Ion chromatography to detect salts in stone structures and to assess salt removal methods. EGU General Assembly Conference Abstracts, 2012, vol. 14, p. 1757.
30. P. Frongia, F. Di Gregorio, G. Piras, Indagini termografiche, trasformazioni architettoniche e degrado dei materiali nelle chiese del centro storico di Siliqua (Sardegna S-W), in: Bollettino della Associazione Italiana di Cartografia, 2013
31. G. Pappalardo, S. Mineo, D. Caliò, A. Bognandi, Evaluation of Natural Stone Weathering in Heritage Building by Infrared Thermography, Heritage 2022, 5, 2594-2614. https://doi.org/10.3390/heritage5030135
32. R.L. Folk, Spectral subdivision of limestone types. Bull. Am. Assoc. Pet. Geol. 1962, 1, 62–84.
33. R.J. Dunham, Classification of Carbonate Rocks According to Depositional Textures. Amer. Ass. Pet. Geol. 1962, 108–121.
34. F. Bozzano, S. Martino, A. Prestininzi, Role of the geological setting on the stability conditions of the Gerace hill (Reggio Calabria, Italy), Italian Journal of Geosciences, 2010, 129. 280-296. DOI:10.3301/IJG.2010.10.
35. O. Petrucci, M. Polemio, Il dissesto della rupe di Gerace: patrimonio artistico e fattori idrogeologici di rischio, Convegno Geoben, Torino, 7-9 Giugno 2000.
36. A.J. Matthew, A. J. Woods, C. Oliver, Spots before the eyes: New comparison charts for visual percentage estimation in archaeological material, in: Recent developments in ceramic petrology, ed. A. Middleton and I. Freestone. London: British Museum Research Laboratory, 1991, 211-64.
37. K. Elert, C. Rodriguez-Navarro, E.S. Pardo, E. Hansen, O. Cazalla, Lime Mortars for the Conservation of Historic Buildings, Studies in Conservation, 2002, 47:1, 62-75, DOI: 10.1179/sic.2002.47.1.62

38. T. Schmid, P. Dariz, Raman Microspectroscopic Imaging of Binder Remnants in Historical Mortars Reveals Processing Conditions. Heritage 2019, 2, 1662-1683. https://doi.org/10.3390/heritage2020102
39. S. Cuezva, J. Garcia-Guinea, A. Fernandez-Cortes, D. Benavente, J. Ivars, J.M. Galan, S. Sanchez-Moral, Composition, uses, provenance and stability of rocks and ancient mortars in a Theban Tomb in Luxor (Egypt). Mater Struct 49, 941–960, 2016. https://doi.org/10.1617/s11527-015-0550-5
40. M.A. Zicarelli, M.F. La Russa, M.F. Alberghina, S. Schiavone, R. Greca, P. Pogliani, M. Ricca, S.A. Ruffolo, A Multianalytical Investigation to Preserve Wall Paintings: A Case Study in a Hypogeum Environment, Materials. 16, 2023, 1380. https://doi.org/10.3390/ma16041380.
41. David Hradil, Tomáš Grygar, Janka Hradilová, Petr Bezdička, Clay and iron oxide pigments in the history of painting, Applied Clay Science, Volume 22, Issue 5, 2003, pp. 223-236, https://doi.org/10.1016/S0169-1317(03)00076-0.
42. D. Hradil, J. Hradilová, P. Bezdička, Clay Minerals in European Painting of the Mediaeval and Baroque Periods, Minerals. 10, 2020, 255. https://doi.org/10.3390/min10030255.
43. D. Hradil, J. Hradilová, P. Bezdička, New Criteria for Classification of and Differentiation between Clay and Iron Oxide Pigments of Various Origins. In: Acta Artis Academica, Proceedings of the 3rd Interdisciplinary ALMA Conference, Prague, Czech Republic, 24–26 November 2010, 107-136. ISBN 978-80-87108-14-7.
44. G. Vasco, A. Serra, D. Manno, G. Buccolieri, L. Calcagnile, A. Buccolieri, Investigations of byzantine wall paintings in the abbey of Santa Maria di Cerrate (Italy) in view of their restoration, Spectrochim. Acta A Mol. Biomol. Spectrosc. 2020, 239, 1386–1425.
45. E. Cheilakou, M. Troullinos, M. Koui, Identification of pigments on Byzantine wall paintings from Crete (14th century AD) using non-invasive Fiber Optics Diffuse Reflectance Spectroscopy (FORS). J. Archaeol. Sci. 2014, 41, 541–555.
46. M. Ricca, M.F. Alberghina, N.D. Houreh, A.S. Koca, S. Schiavone, M.F. La Russa, L. Randazzo, S.A. Ruffolo, Preliminary Study of the Mural Paintings of Sotterra Church in Paola (Cosenza, Italy), Materials. 15, 2022, 3411. https://doi.org/10.3390/ma15093411.
47. C. Crova, F. Miraglia, La termografia come strumento di indagine conoscitiva delle superfici architettoniche. Interventi e prospettive di ricerca, in Intervenire sulle superfici dell'architettura tra bilanci e prospettive, 34° Convegno Internazionale Scienza e Beni Culturali, Collana Scienza e Beni Culturali, 2018
48. S.J.C. Granneman, B. Lubelli, R.P.J. van Hees, Effect of mixed in crystallization modifiers on the resistance of lime mortar against NaCl and Na2SO4 crystallization. Construct. Build. Mater., 2019, 194, pp. 62-70.
49. A. Arnold, K. Zehnder, Monitoring Wall Paintings Affected by Soluble Salts, in: The Conservation of Wall Paintings: Proceedings of a symposium organized by the Courtauld Institute of Art and the Getty Conservation Institute, London, July 1987, 521 13-16, pp. 103-132
50. L. Germinario, C. T. Oguchi, "Underground salt weathering of heritage stone: lithological and environmental constraints on the formation of sulfate efflorescences and crusts", Journal of Cultural Heritage Volume 49, May–June 2021, pp. 85-93
51. T. Díaz Gonçalves, J. Delgado Rodrigues, M. Marinho Abreu, "Evaluating the salt content of salt-contaminated samples on the basis of their hygroscopic behaviour: Part II: experiments with nine common soluble salts", Journal of Cultural Heritage Volume 7, Issue 3, July–September 2006, pp. 193-200
52. I.S. Evans, Salt crystallization and rock weathering: A review. Rev. Géomorphol. Dyn. 1970, 19, 153–177
53. E.M. Winkler, Stone, in: Architectur, 1st ed.; Springer: Berlin/Heidelberg, Germany, 1994
54. A.S. Goudie, H.A. Viles, Salt Weathering Hazard, 1st ed.; Wiley: London, UK, 1997
55. C. Rodriguez-Navarro, Doehne, E. Salt weathering: Influence of evaporation rate, supersaturation and crystallization pattern. Earth Surf. Process. Landf. 1999, 24,191–209

Chapter 3

In the third chapter, the attention has been laid on another aspect of preventive conservation: the application of a protective coating. The preliminary results of the development of a new coating suitable for the conservation of underwater cultural heritage will be showed. This work takes place in the framework of the TECTONIC project (EU-H2020-MSCA-RISE-2019873132-TECTONIC Technological Consortium TO develop sustainability of underwater Cultural heritage) [27], as a collaboration between the University of Calabria (Italy) and Synpo akciova spolecnost (Czech Republic).

This chapter has been published as:
Donato, A., Novàk, M., Novàkovà, M., La Russa, M.F., Ruffolo, S.A., Ricca, M. (2023). A Preliminary Study of Unconventional Coatings for the Conservation of Underwater Cultural Heritage Within the TECTONIC Project. In: Mehmood, R., et al. Distributed Computing and Artificial Intelligence, Special Sessions I, 20th International Conference. DCAI 2023. Lecture Notes in Networks and Systems, vol 741. Springer, Cham. https://doi.org/10.1007/978-3-031-38318-2_21

Abstract: Underwater Cultural Heritage (UCH) refers to all the traces of human existence that are located underwater. These can include shipwrecks, submerged buildings, and other archaeological sites. The conservation of UCH can be challenging due to the unique environmental conditions, the difficulty of accessing and working in underwater environments, as well as the potential for damage from natural forces and human activity. The TECTONIC project aims to promote an intersectoral collaboration between academic and non-academic professionals, supporting the exchange of skill and expertise between them, aiming to implement, improve and assess innovative materials, techniques, tools, and methodologies for the Underwater Cultural Heritage. In this framework, the technology and scientific exchange between the University of Calabria (Italy) and Synpo akciova spolecnost (Czech Republic), is leading to the preparation of an underwater coating with antifouling properties suitable for the protection of underwater cultural heritage.

Keywords: Underwater, Cultural heritage, Coating, Epoxy Resin.

1. Introduction

In recent decades, there has been a growing interest in studying degradation phenomena that occur at underwater archaeological sites. Various research efforts have focused on both the degradation of stone materials in underwater environments and on developing innovative approaches for their protection [1-5].
One of the most significant forms of damage to submerged archaeological artifacts is biological colonization (bio-fouling), which can develop differently depending on a variety of environmental conditions, as well as the textural and structural features of the materials [1,4,6,7].
The latest guidelines from scientific and international cultural heritage protection organizations support the promotion, protection, and in-situ preservation of underwater archaeological and historical heritage, as outlined in the UNESCO Convention on the Protection of the Underwater Cultural Heritage from November 2nd, 2001.
Epoxy resins find numerous applications due to their desirable properties. They are widely used as adhesives, coatings, and sealants in various industries, from the construction sector [8] to the electronics and crafts industry. Applications of resin for stabilization and restoration of Cultural Heritage can be found in literature [9,10]. The present research, which is a part of the TECTONIC project (EU-H2020-MSCA-RISE-2019-873132-TECTONIC TEchnological Consortium TO develop sustaiNabIlity of underwater Cultural heritage), aims to develop an epoxy resin-based system with antifouling properties for the conservation and preservation of underwater stone materials [11].
The work is still in progress and therefore only the preliminary results based on the initial stages of laboratory experimentation will be discussed in the next paragraphs.

2. Material and Methods

Epoxy resin is a type of thermosetting polymer that is formed through the reaction of an epoxy resin and a curing agent. It is a versatile material known for its excellent adhesive properties, high strength, and chemical resistance [12-13]. Typically, they are made by combining two components: an epoxy resin and a curing agent. The epoxy resin, also known as the "resin component," is a viscous liquid that contains epoxy groups. The curing agent, also called the "hardener," is a chemical compound that reacts with the epoxy resin, leading to cross-linking and the formation of a three-dimensional network. Once the epoxy resin and curing agent are mixed, a chemical reaction known as polymerization occurs. This curing process can be accelerated by the addition of heat or a catalyst. This reaction results in the formation of strong covalent bonds, creating a rigid and durable material. The cured epoxy resin has excellent mechanical properties, including high tensile and compressive strength, as well as good resistance to chemicals, moisture, and temperature extremes.
The first step of the research focused on a screening of the various epoxy resin-based systems produced by Synpo, trying to find out the most suitable and compatible formulation for underwater application. The products have been divided into series, according to the type of resin and the additives used. The colorimetric tests, the measurement of the contact angle, viscosity and underwater applicability were therefore evaluated, while the antifouling and ecotoxicity tests are still in progress. The products were applied on marble and limestone specimens sized 5x5x2 cm, in order to evaluate any different performance of the coatings on the lithotypes most commonly used in the field of cultural heritage.
Color variations induced by the treatment were evaluated by means of colorimetric tests [14], using a CM-2600d Konica Minolta spectrophotometer. Chromatic values are expressed in the CIE L*a*b* space, where L* is the lightness/darkness coordinate, a* the red/green coordinate (+a* indicating red and −a* green) and b* the yellow/blue coordinate (+b* indicating yellow and −b* blue).
Contact angle measurements [15] was carried out in order to determine the wettability of the treated surface, as this parameter may influence the adhesion of microorganisms in the submerged

environment. The measurement consisted in the placement of a water drop of defined volume on the solid sample surface. Drop shape was recorded with a camera and automatically evaluated in terms of contact angle, which represents the angle between the substrate surface and the tangent from the edge to the contour of the drop.
Viscosity tests were carried out by Brookfield DV-II+Pro RV viscometer, coupled with Vane V-74 spindle, in order to obtain information about the behavior of the compound under various shear rates.
Underwater applicability was evaluated using standardized two-component cartridges with a static mixer to obtain correctly mixed system under water-free conditions. Premixed coating was hereafter spread by various tools (brush, sponge, spatula) in an aquarium. It's important to note that for underwater tests, the original formulation was modified adding an UV-sensitive pigment, in order to check whether the product was well applied or not. The addition of this pigment did not alter any final thermos-mechanical property of the product.
In the next paragraphs, the discussion will be limited to the series of samples that proved to be suitable after the initial screening, that is Cx series, characterized by a modification of epoxy resin by thixotropic agent.

3. Results and Discussion

In order to narrow down the number of products to use in the research, a preliminary hydrophobicity test was carried out. Various types of epoxy resins and hardeners were placed in a container with water and mixed to observe their degree of immiscibility in water. The most immiscible samples, i.e., those that separated most rapidly from the water in a separate layer, keeping it clear, were subjected to further testing. This behavior ensures that mixed will not be dissolved to the environment when applied on the protected cultural heritage. Secondly, the selected epoxy resin and hardener were modified by thixotropic agents to improve rheological properties that suits underwater application. The aim of this modification was to find out the products with a pseudoplastic behavior. This behavior refers to a type of non-Newtonian fluid behavior where the viscosity of a material decreases as the shear rate or deformation rate increases. This means that the material becomes less resistant to flow as the applied force or stress increases. This character of resin ensures easy application on the sample and eliminates wash-out to the environment when the coating is applied. The C7 sample from Cx series modified with thixotropic agent, appeared to be the most suitable product (Fig. 1).

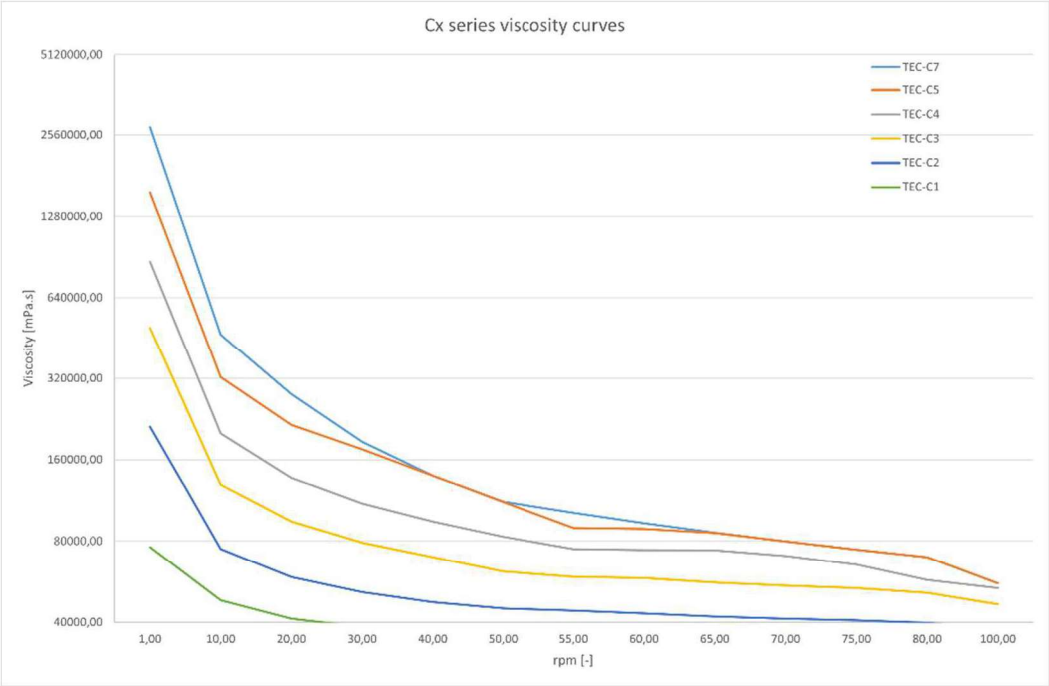

Fig. 1. Viscosity test results for Cx series.

Hardener (B2) was chosen such that its viscosity curve was the closest matching one that of the selected resin: a modification of hardener by thixotropic agent (Fig. 2).

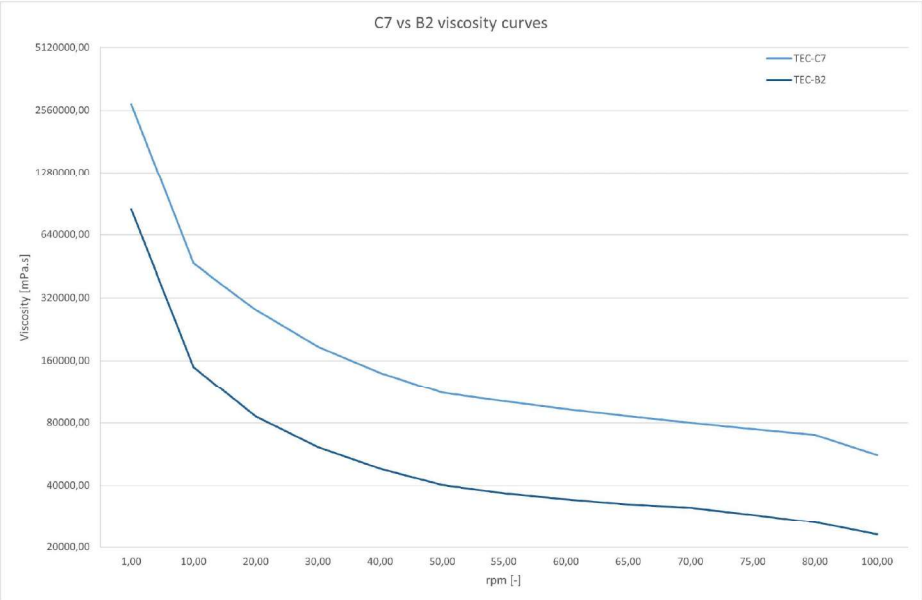

Fig. 2. C7 vs B2 viscosity curves.

For what concerns colorimetric variation, we can notice a different behavior depending on the lithotype used: negligible variation for marble specimens and important color changes for limestone ones (Tab. 1).

Table 1. Colorimetric test results.

Colorimetric Measurements					
Lithotype	**Reference value**		**After treatment**		**ΔE**
Marble	L*	79.1	L*	77.4	1.7
	a*	-1.1	a*	-1.4	
	b*	1.0	b*	0.8	
Limestone	L*	82.7	L*	72.2	13.8
	a*	0.3	a*	1.2	
	b*	7.2	b*	16.4	

Contact angle measurement showed an increase in hydrophobicity, which should decrease the adhesion capability of microorganisms in a marine environment; further confirmation or denial will come from bacterial tests.

Table 2. Contact angle results.

Contact angle Measurements		
Lithotype	**Reference value**	**After treatment**
Marble	50.86	69.3
Limestone	21.20	68.6

The underwater applicability tests focused on several aspects: possible dispersion of the product during application, ease of application depending on the tool used, and hardening of the product. The results confirmed what had previously emerged from the viscosity tests: C7 sample showed the best applicability in the underwater environment, using soft brushes and/or sponges (Fig. 3), even though issues with short pot life of the mixed product (resin + hardener) emerged.

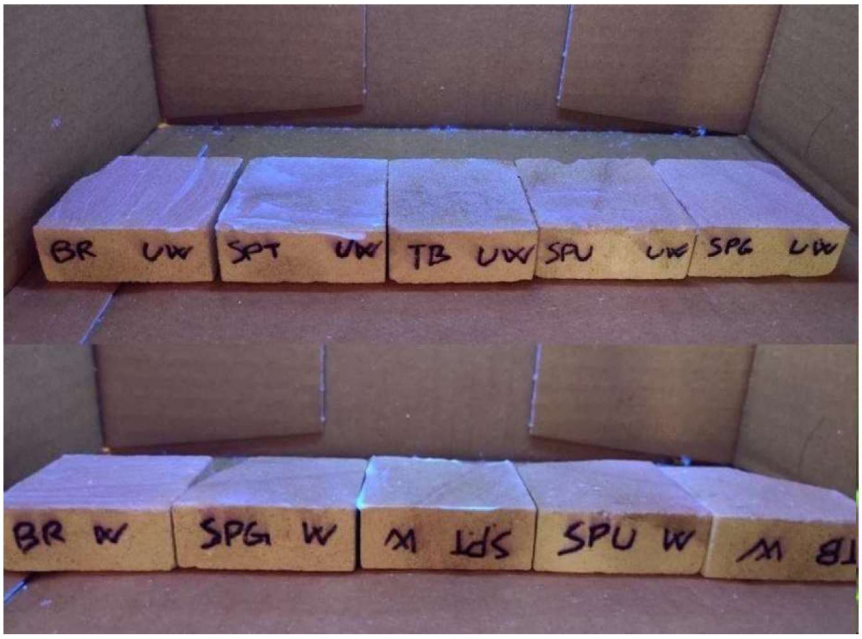

Fig. 3. Different application methods on limestones for C7 product. W=wet samples, on air application; UW=underwater application; BR=brush, SPT=spatula, TB=toothbrush, SPU=PVA sponge, SPG=sponge.

4. Conclusions

The research carried out in the frame of the TECTONIC project is still in progress, but the preliminary results are well promising. Colorimetric test showed negligible color variation on marble and significant color change on limestone that was caused by high gloss of the coating. The development of protective coating still continues and current studies are focused on the incorporation of a matting agent in order to reduce color variation on limestone samples. Also, further tests on wet samples will be performed to provide an evaluation representing marine environment. Contact angle measurements showed the increase in hydrophobicity of the treated surface, which will, hopefully, discourage the growth of microorganism on it. Adjustments need to be done on formulation to slow down the pot life of the product, without altering the current other properties. The next stages of laboratory experimentation will focus on antifouling tests on the already formulated products in order to guarantee their use for the protection of underwater objects and stone materials of cultural interest.

References

1. Ricci, S., Davidde, B., Bartolini, M., Priori, G.F.: Bioerosion of lapideous artefacts found in the underwater archaeological site of Baia (Naples), Archaeol. Marit Mediterr. Int. J. Underw. Archaeol. 6 (2009) 167–186.
2. Crisci, G.M., La Russa, M.F., Macchione, M., Malagodi, M., Palermo, A.M., Ruffolo, S.A.: Study of archaeological underwater finds: deterioration and conservation, Appl. Phys. A 100 (2010) 855–863.
3. La Russa, M.F., Ruffolo, S.A., Ricci, S., Davidde, B., Barca, D., Ricca, M., Capristo, V.: A Multidisciplinary approach for the study of underwater artefacts: the case of Tritone Barbato marble statue (Grotta Azzurra, Island of Capri, Naples), Period Miner. 82 (2013) 101–111.
4. La Russa, M.F., Ricca, M., Belfiore, C.M., Ruffolo, S.A., Álvarez Ballester De Buergo, M., Crisci, G.M.: The contribution of earth sciences to the preservation of underwater archaeological stone materials: an analytical approach, Int. J. Conserv. Sci. 6 (2015) 335–348.
5. La Russa, M.F., Ruffolo, S.A., Ricca, M., Rovella, N., Comite, V., Barca, D.: Archaeometric approach for the study of mortars from the underwater archaeological site of Baia (Naples) Italy: preliminary results, Period Miner. 84 (2015) 1–16.
6. Davidde, B., Ricci, S., Poggi, D., Bartolini, M.: Marine bioerosion of stone artefacts preserved in the museo archeologico dei Campi Flegrei in the castle of Baia (Naples), Archaeol. Marit Mediterr. Int. J. Underw. Archaeol. 7 (2009) 75–115.
7. Relini, G.: Il Biofouling, Biol. Marit Mediterr. 10 (2003) 285–326.
8. Dębska, B.; Brigolini Silva, G.J. Mechanical Properties and Microstructure of Epoxy Mortars Made with Polyethylene and Poly(Ethylene Terephthalate) Waste. Materials 2021. 14 (9): 2203. doi:10.3390/ma14092203.
9. The Application of Epoxy Resins for the Restoration of Historic Structures. Bulletin of the Association for Preservation Technology 3, no. 1 (1971): 59–63.
10. Selwitz, C. The Use of Epoxy Resins for the Stabilization of Deteriorated Masonry. APT Bulletin: The Journal of Preservation Technology 26, no. 4 (1995): 27–34. https://doi.org/10.2307/1504447.
11. Ricca, M., Alexandrakis, G., Bonazza, A., Bruno, F., Davidde Petriaggi, B., Elkin, D., Lagudi, A., Nicolas, S., Novák, M., Papatheodorou, G., Prieto, J., Ricci, M., Vasilijevic, A., Francesco La Russa, M. A Sustainable Approach for the Management and Valorization of Underwater Cultural Heritage: New Perspectives from the TECTONIC Project. Sustainability 2020, 12, 5000. https://doi.org/10.3390/su12125000.
12. Capricho, J.C., Fox, B., Hameed, N. Multifunctionality in Epoxy Resins. Polymer Reviews 2020. 60 (1): 1–41. doi:10.1080/15583724.2019.1650063.
13. Ruffolo, S.A., Ricca, M., Macchia, A., La Russa, M.F. Antifouling coatings for underwater archaeological stone materials, Progress in Organic Coatings, 104, 2017: 64-71. https://doi.org/10.1016/j.porgcoat.2016.12.004.

14. NorMaL 43/93: misure colorimetriche di superfici opache. Raccomandazioni NorMaL: alterazioni dei materiali lapidei e trattamenti conservativi: proposte per l'unificazione dei metodi sperimentali di studio e di controllo. Roma, Italy: CNR 1993.
15. NorMaL 33/89: misura dell'angolo di contatto. Raccomandazioni NorMaL: alterazioni dei materiali lapidei e trattamenti conservativi: proposte per l'unificazione dei metodi sperimentali di studio e di controllo. Roma, Italy: CNR 1989.

General Conclusions

The multidisciplinary approach employed, and focus of my PhD research, has demonstrated his validity as good practice in the preventive conservation of cultural heritage.
In both case studies, the swift assessment of the state of conservation of cultural assets has been a crucial support to institutions and restorers in the planning of future interventions.
In particular, on Cosenza Cathedral allowed to define a priority scale of intervention on the façade, giving support to institutions in terms of time and resources management.
As far it concerns Gerace Cathedral, this work provided useful information to restores allowing the choice of the right procedures to enable a proper restoration, due to the lack of data in literature about building materials and their state of conservation.
Overall, in both cases, this approach has demonstrated how important the choice of methodologies is when dealing with an advanced state of deterioration and a prompt restoration intervention is required.
Even in underwater environment where the decay agents responsible of CH degradation are different from sub-aerial ones, the multidisciplinary method applied enabled the fundamentals for a first approach to the formulation of a new protective coating. As UCH is part of humankind's history and traditions, it must be preserved. New and more efficient solutions must be found for its safeguard while ensuring its accessibility for a future valorization.

Supplementary Material

Table S1. Polarising optical microscopy: synthesis of data. Cal = calcite; Qtz = quartz; Fsp = feldspars; Mic = micas; Ox = oxides; Px = pyroxene; Car = carbonatic rocks; Met = metamorphic rocks; Vol = volcanic rocks; Cocc = cocciopesto; S = sorted; M = moderately; P = poor; PS = poorly sorted; WS = well sorted; micr = micritic; crypt = cryptocrystalline; c/f/v ratio (%): coarse fraction/fine fraction/vughs = groundmass/aggregate/pore ratio. S = Type Stone Materials/Group 1; M = Type Mortars/Group 2; P/PF = Type Plasters/Pictorial Film. Note: as for the c/f/v ratio (%), the semi-quantitative estimation was carried out by visual valuation, and always following "G. Pappalardo, S. Mineo, D. Caliò, A. Bognandi, Evaluation of Natural Stone Weathering in Heritage Building by Infrared Thermography, Heritage 2022, 5, 2594-2614. https://doi.org/10.3390/heritage5030135"

Sample Id	Type /Group	Layers	Groundmass /Binder	Predominant inclusions	Other inclusions	Size of inclusions (μm)	Rock fragments	Other fragments	Size of rock fragments (μm)	Sorting	Common grain shape	c/f/v ratio (%)
G1	M	A	micr	Qtz; Mic; Cal; Bioclasts	Fsp; Px; Ox	Up to 500	Met; Car; Vol	Cocc	up to 2100	S to M	medium-low sphericity, from sub-angular to rounded	40/50/10
		B	micr	Qtz; Mic; Cal	Bioclasts	Up to 400	Vol	/	Up to 500	PS	medium-low sphericity, from angular to sub-rounded	20/70/10
G2	M	A	micr	Qtz; Mic; Cal; Bioclasts	Fsp; Px; Ox	Up to 1500	Car; Vol	Cocc	Up to 1600	S to M	medium-low sphericity, from angular to sub-rounded	40/50/10
		B	micr	Qtz; Cal	/	Up to 500	/	/		PS	medium-low sphericity, from sub-angular to sub-rounded	10/85/5
G3	M	A	micr	Qtz; Mic; Cal; Bioclasts	Fsp; Px; Ox	Up to 900	Met; Car; Vol	/	Up to 2300	WL	medium-low sphericity, from angular to sub-rounded	40/50/10
		B	micr	Qtz; Cal	Mic; Bioclasts; Ox	Up to 400	Car; Vol	/	Up to 400	S	medium-low sphericity, from angular to sub-rounded	45/50/5
G4	M	A	micr	Qtz; Mic; Cal; Bioclasts	Fsp; Ox	Up to 1300	Car; Vol	Cocc	Up to 2800	P to S	medium-low sphericity, from sub-angular to rounded	65/35/5
G5	S	/		Qtz; Mic; Cal; Bioclasts	Ox	Up to 1000	Met; Car; Vol	/	Up to 2800	WS	medium-low sphericity, from sub-angular to rounded	40/45/15
G6	M	A	micr	Qtz; Mic; Cal; Bioclasts	Fsp; Ox	Up to 600	Met; Car; Vol	/	Up to 1750	P to M	medium-low sphericity, from sub-angular to rounded	50/40/10
G7	P/PF	A	micr	Qtz; Mic; Cal; Bioclasts	Fsp; Ox	Up to 850	Met; Car; Vol	/	Up to 4050	WS	medium-low sphericity, from angular to sub-rounded	40/45/15
		B	micr	Qtz; Cal	/	/	/	/	/	/	/	0/95/5

G8	P/PF	A	micr/crypt	Qtz; Mic; Cal; Bioclasts	Fsp; Ox	Up to 1200	Met; Car; Vol	Cocc	Up to 4000	S to M	medium-low sphericity, from angular to sub-rounded	45/50/5
		B	pigment	Ox	/	/	/	/	/	/	/	/
		C	scialbo	Cal	/	/	/	/	/	/	/	/
G9	P/PF	A	micr/crypt	Qtz; Mic; Cal; Bioclasts	Fsp; Ox	Up to 700	Met; Car; Vol	/	Up to 1750	P to M	medium-low sphericity, from sub-angular to rounded	50/40/10
		B	pigment	Ox	/	/	/	/	/	/	/	/
G10	P/PF	A	micr	Qtz; Cal	Bioclasts, Fsp; Ox	Up to 500	Car; Vol	/	Up to 2800	PS	medium-low sphericity, from angular to sub-rounded	30/65/5
		B	pigment	Ox	/	/	/	/	/	/	/	/
		C	scialbo	Cal	/	/	/	/	/	/	/	/
G11	P/PF	A	micr	Qtz; Cal	Bioclasts; Ox	Up to 1400	Car; Vol	/	Up to 1000	PS	medium-low sphericity, from angular to sub-rounded	20/70/10
		B	pigment	Ox	/	/	/	/	/	/	/	/
		C	scialbo	Cal	/	/	/	/	/	/	/	/
G12	P/PF	A	micr/crypt	Qtz; Cal	Fsp; Mic; Ox	Up to 650	Car; Vol; Met	/	Up to 1500	P to M	medium-low sphericity, from angular to sub-rounded	30/65/5
		B	pigment	Ox	/	/	/	/	/	/	/	/
G13	P/PF	A	micr	Qtz; Cal	Fsp; Mic; Ox	Up to 700	Car; Vol; Met	/	Up to 650	P to M	medium-low sphericity, from angular to sub-rounded	30/65/5
		B	pigment	Ox	/	/	/	/	/	/	/	/
G14	P/PF	A	micr	Qtz; Mic; Cal; Bioclasts	Ox	Up to 1000	Vol; Car	Cocc	Up to 1700	P to M	medium-low sphericity, from angular to sub-rounded	50/40/10
		B	pigment	Ox	/	/	/	/	/	/	/	/
		C	scialbo	Cal	/	/	/	/	/	/	/	/
G15	P/PF	A	micr	Qtz; Mic; Cal; Bioclasts	Ox	Up to 800	Vol; Car	/	Up to 1000	P to M	medium-low sphericity, from angular to sub-rounded	40/45/15
		B	pigment	Ox	/	/	/	/	/	/	/	/
G16	P/PF	A	micr	Qtz; Mic; Cal; Bioclasts	Ox	Up to 750	Car; Vol	/	Up to 1200	P to M	medium-low sphericity, from angular to sub-rounded	50/40/10

		B	pigment	Ox	/	/	/	/	/	/	/	/
G17	P/PF	A	micr	Qtz; Mic; Cal; Bioclasts	Ox	Up to 800	Car; Vol	/	Up to 2200	P to M	medium-low sphericity, from angular to sub-rounded	30/65/5
		B	pigment	Ox	/	/	/	/	/	/	/	/
G18	P/PF	A	micr	Qtz; Mic; Cal; Bioclasts	Ox	Up to 600	Car; Vol	Cocc	Up to 1950	P to M	medium-low sphericity, from angular to sub-rounded	30/65/5
		B	pigment	Ox	/	/	/	/	/	/	/	/
G26	S	/	/	Cal	/	/	/	/	/	/	/	/
G27	S	/	/	Cal	/	/	/	/	/	/	/	/
G29	S	/	/	Cal	/	/	/	/	/	/	/	/
G31	P/PF	A	micr	Qtz; Mic; Cal; Bioclasts	Ox	Up to 950	Car; Vol; Met	/	Up to 1300	S to M	medium-low sphericity, from sub-angular to rounded	50/40/10
		B	pigment	Ox	/	/	/	/	/	/	/	/
		C	scialbo	Cal	/	/	/	/	/	/	/	/
G32	P/PF	A	micr	Qtz; Mic; Cal; Bioclasts	Ox	Up to 800	Car; Vol; Met	/	Up to 1600	S to M	medium-low sphericity, from sub-angular to rounded	50/40/10
		B	pigment	Ox, Cal	/	/	/	/	/	/	/	/
G33	P/PF	A	micr	Qtz; Mic; Cal; Bioclasts	Ox	Up to 850	Car; Vol; Met	/	Up to 1400	S to M	medium-low sphericity, from sub-angular to rounded	50/40/10
		B	pigment	Ox	/	/	/	/	/	/	/	/